Survival secrets of mistletoes: high drought tolerance in canopy habitats

Article *in* Tree Physiology · June 2025

DOI: 10.1093/treephys/tpaf071

11 authors, including:

Yunbing Zhang
Xishuangbanna Tropical Botanical Garden
22 PUBLICATIONS **229** CITATIONS
SEE PROFILE

Marina Corrêa Scalon
Federal University of Paraná
48 PUBLICATIONS **2,229** CITATIONS
SEE PROFILE

Yan Ke
Chinese Academy of Sciences
8 PUBLICATIONS **41** CITATIONS
SEE PROFILE

Da Yang
Chinese Academy of Sciences
29 PUBLICATIONS **366** CITATIONS
SEE PROFILE

Tree Physiology, 2025, **45**, tpaf071
https://doi.org/10.1093/treephys/tpaf071
Advance access publication date 18 June 2025
Research paper

Survival secrets of mistletoes: high drought tolerance in canopy habitats

Xian-Yan Huang[1,2], Yun-Bing Zhang[1,*], Marina Corrêa Scalon[3], Yan Ke[1,4], Wen-Hua Li[1], Da Yang[1], Amy N. A. Aritsara[1], Yong-Jiang Zhang[5,6], Zheng-Lin Wan[7], Xiao-Li Cheng[2] and Jiao-Lin Zhang[1,*]

[1]CAS Key Laboratory of Tropical Forest Ecology, Xishuangbanna Tropical Botanical Garden, Chinese Academy of Sciences, Menglun, Mengla, Yunnan 666303, China
[2]School of Ecology and Environmental Science, Yunnan University, Kunming, Yunnan 650500, China
[3]Programa de Pós-graduação em Ecologia e Conservação, Universidade Federal do Paraná, Curitiba, PR 81531-990, Brazil
[4]University of Chinese Academy of Sciences, Beijing 100049, China
[5]School of Biology and Ecology, University of Maine, Orono, ME 04469, USA
[6]Climate Change Institute, University of Maine, Orono, ME 04469, USA
[7]Menglun Administration of Xishuangbanna National Nature Reserve, Menglun, Mengla, Yunnan 666303, China

*Corresponding authors (zhangjiaolin@xtbg.ac.cn; zhangyb@xtbg.org.cn)

Handling Editor: José Torres-Ruiz

The interaction between mistletoes and hosts impacts tree performance and mortality under climate change. However, little is known about the hydraulic performance and drought resistance of mistletoes, and their potential impacts on hosts. Here, we measured 21 functional traits related to hydraulics and drought resistance of eight mistletoe–host species pairs. We found that mistletoes were more drought tolerant compared with their hosts, characterized by more negative midday leaf water potentials during the dry season, turgor loss point (ranging from −1.81 to −2.48 MPa) and water potential at 12% loss of conductivity (ranging from −0.97 to −2.94 MPa), higher Huber values, sapwood density and vessel density, and lower leaf size, specific leaf area, vein density and stomatal density. Meanwhile, mistletoes were less hydraulically efficient compared with their hosts, demonstrated by lower leaf-specific hydraulic conductivity, sapwood-specific hydraulic conductivity and hydraulically weighted vessel diameter. Paradoxically, mistletoes showed lower water-use efficiency (as indicated by more negative stable carbon isotope values). Notably, trait associations between mistletoes and hosts differed, with mistletoes showing stronger correlations among functional traits, both within leaf traits and between leaf and stem traits. This suggests divergent ecological strategies between mistletoes and their hosts. However, no trade-off between hydraulic efficiency and safety was observed across the mistletoes and hosts examined. High plasticity in hydraulic traits was also found in mistletoes, with water potential at 12, 50 and 88% loss of conductivity varying significantly and intraspecifically across host species. Furthermore, trait correlations in mistletoes were driven by both intraspecific and interspecific variation, with interspecific variation being more important. These findings highlight the response capacity of mistletoes, enabling them to adjust their hydraulic strategies based on host-specific conditions. This study provides insights into mistletoe water use, drought resistance and potential responses to changing environmental conditions.

Keywords: embolism resistance, functional traits, hemiparasitic plants, hydraulics, profligate water use, xylem anatomy.

Introduction

Recent decades have seen a rise in extreme drought events and heatwaves (Dai 2013, Bauman et al. 2022), causing widespread plant diebacks and increasing tree vulnerability to parasites like mistletoes, thereby escalating tree mortality (Griebel et al. 2017, Anderegg et al. 2020, Maponga et al. 2021). Vulnerable to prolonged droughts, mistletoes face the risks of host depletion and potential extinction (Bell et al. 2020, Crates et al. 2022, Griebel et al. 2022). The death of mistletoes can trigger cascading effects on community composition and ecosystem functioning, such as pollination and seed dispersal (Fontúrbel et al. 2018, Crates et al. 2022). Mistletoes also provide habitat, shelter and food for animals, promote nutrient cycling, enhance plant productivity and maintain biodiversity (Mellado et al. 2016, Ndagurwa et al. 2020, Těšitel et al. 2021). As such, they are considered keystone species and ecosystem engineers (Watson and Herring 2012). Given the significant ecological impacts of mistletoes, the interactions between mistletoes and their hosts have become a hot topic in recent years (e.g., Mellado et al. 2019, Watson et al. 2022, Zhang et al. 2023, 2025). However, little is known about how mistletoes adjust their hydraulics to their unique canopy environment compared with their hosts.

Mistletoes are obligate stem hemiparasitic plants, which are capable of photosynthesis but absorb water and mineral nutrients from their hosts through haustoria (Glatzel and Geils 2009, Teixeira-Costa 2021). Mistletoes and their hosts are hydraulically connected, with the movement of xylem sap from the host to the mistletoe, requiring a water potential gradient between them (Glatzel and Geils 2009). To maintain this gradient and avoid stomatal closure or wilting, mistletoes must tolerate lower leaf water potentials than their hosts (Goldstein et al. 1989, He et al. 2021, Ye et al. 2021), along with higher stomatal conductance and transpiration rates

Received: November 12, 2024. **Accepted:** June 13, 2025

(Zweifel et al. 2012, Yang et al. 2017). This may impose various constraints and costs, such as the need to invest in embolism resistance (Bucci et al. 2003, Nardini et al. 2011, Jin et al. 2023). Additionally, mistletoes, particularly those growing on exposed branches, may experience slightly higher evaporative demand due to differences in boundary layer dynamics and exposure, meanwhile showing a profligate water-use strategy (Scalon and Wright 2015, Zhang et al. 2023). It remains unclear how mistletoes adapt to their habitat, and how they maintain such a lower water-use efficiency. Previous studies have mainly focused on the influences of mistletoe infection on host physiology, growth and community dynamics (Griebel et al. 2021, Amutenya et al. 2023, de Andrés et al. 2024), diversity and distribution patterns (Luo et al. 2015, Sayad et al. 2017, Zhang et al. 2018) and photosynthesis, water and nutrient interaction between mistletoes and their hosts (Chen et al. 2013, Zhang et al. 2023). However, the functional traits of mistletoes, especially stem traits, have received relatively limited attention compared with non-parasitic plants (Haynes 2021, Teixeira-Costa et al. 2023, Zhang et al. 2025).

Plant functional traits are anatomical, morphological, physiological, chemical and phenological characteristics that directly affect plant survival, growth and fitness (Violle et al. 2007), and are often used to reflect plant adaptation to the environments and their ecological strategies (Wright et al. 2007, Reich and Cornelissen 2014, Skelton et al. 2015). Plants employ different ecological strategies to adapt to their environments, with the specific mechanisms favored depending on how they access and compete for resources (Carvajal et al. 2019, Pérez-Ramos et al. 2019). For example, plants living in dry conditions may have higher leaf dry matter content (LDMC), stem embolism resistance and Huber value (HV), but lower specific leaf area (SLA), sapwood-specific hydraulic conductivity and water potential at the leaf turgor loss point (TLP) to better cope with water deficit (Zweifel et al. 2012, Mencuccini et al. 2019, Haverroth et al. 2024). In addition, functional traits are correlated (coordination and/or trade-off) to adapt to the environment due to biophysical and/or evolutionary constraints (Westoby et al. 2002, Wright et al. 2007, Chave et al. 2009), which reflects the differences in life-history and ecological strategy among species. For instance, the trade-offs between hydraulic efficiency and hydraulic safety have been suggested to play an important role in drought adaptation, spatial distribution and hydraulic strategies among co-occurring species (van der Sande et al. 2019, Liu et al. 2024, Zhang et al. 2024), despite its generality still being debated (Gleason et al. 2016, Liu et al. 2021). In addition, previous studies have found that stem and leaf traits are coordinated to better adapt to the harsh environment (Fu et al. 2012, Shen et al. 2019, Zhang et al. 2022). However, how traits are correlated in mistletoes and whether these relationships differ from those of their hosts have yet to be fully explored, especially considering stem traits.

In this study, we compared 7 stem traits and 14 leaf traits related to hydraulics and drought resistance of eight mistletoe–host species pairs. Our main objective was to assess differences in drought resistance traits between mistletoes and their hosts. We aimed to answer the following two questions and test the corresponding hypotheses: (i) Are there differences in stem and leaf functional traits related to drought resistance between mistletoes and their host plants? We hypothesize that mistletoes have lower water-use efficiency due to their unique water acquisition strategy. Positioned in the host canopy, mistletoes are exposed to high xylem tension (lower water potentials) and exhibit higher stomatal conductance and transpiration (Zweifel et al. 2012, He et al. 2021). Further, mistletoes have a xylem structure that is more embolism-resistant than that of their hosts (Zhang et al. 2025). Therefore, we hypothesize that mistletoes exhibit lower hydraulic efficiency due to their embolism-resistant xylem structures and higher drought tolerance (e.g., more negative xylem water potential at 50% loss of hydraulic conductivity and leaf TLP) to adapt to the canopy habitat while maintaining stomatal opening. (ii) How do mistletoe functional traits correlate with each other? Do these trait relationships differ between mistletoes and hosts? Given that mistletoes may require greater embolism resistance under lower water potentials, we hypothesize that there is a trade-off between hydraulic efficiency and hydraulic safety. Additionally, we predict that stem and leaf traits are coordinated to better cope with the canopy environment, increasing the survival probability of mistletoes.

Materials and methods

Study site and plant material

This study was conducted at the Xishuangbanna Tropical Botanical Garden (21°54′ N, 101°46′ E, elevation 570 m a.s.l.) in southern Yunnan, Southwest China. The mean annual temperature and mean annual precipitation are 22.7 °C and 1557 mm, respectively. This region experiences a distinct dry season from November to April and a wet season from May to October, which contributes over 80% of the yearly rainfall (Cao et al. 2006). It is influenced not only by the weakening of the Indian Ocean monsoon but also mainly by the hot, dry continental winds from the southwest, a southern branch of the westerly circulation. Situated at the southeastern edge of the Himalayas, near the confluence of tropical and temperate zones, the area supports complex habitats and a rich diversity of flora, including numerous parasitic and epiphytic plants (Zhu 2022).

In this study, three mistletoes species, *Dendrophthoe pentandra*, *Scurrula chingii* var. *yunnanensis* and *Viscum ovalifolium*, were selected along with their respective host plants, forming eight unique mistletoe–host species pairs (Table 1). *D. pentandra* and *S. chingii* var. *yunnanensis* belong to the Loranthaceae family, while *V. ovalifolium* is a member of the Santalaceae family. These mistletoe species exhibit distinct differences in morphology, host preference and ecological strategies. Specifically, *D. pentandra* is a generalist with a broad host range, *S. chingii* var. *yunnanensis* is relatively generalist but exhibits some host preferences, whereas *V. ovalifolium* is a specialist mistletoe with a higher degree of host specificity. The host species selected for this study represent a diverse range of leaf habit, including both evergreen and deciduous species. These hosts are primarily tropical plants, including tree, shrub and lianas, which thrive in tropical monsoon climate. Detailed information on their leaf habits is provided in Table 1. All mistletoe species in this study are evergreen.

For each species pair, three individuals from three different trees were sampled. From each sampled mistletoe, two healthy branches were selected, and branch samples from the host tree, free from mistletoe infection, were collected. A total of 7 stem functional traits and 14 leaf functional traits were measured (Table 2). All stem hydraulic measurements and leaf sampling

Table 1. Three mistletoe and eight host species selected in this study.

Mistletoe	Family	Code	Host	Code	Family	Leaf habit
Dendrophthoe pentandra (L.) Miq.	Loranthaceae	Dp	*Elaeagnus conferta* Roxb.	Ec	Elaeagnaceae	Evergreen
			Microcos paniculata L.	Mpa	Malvaceae	Evergreen
			Monoon simiarum (Buch.-Ham. ex Hook. f. & Thomson) B. Xue & R. M. K. Saunders	Ms	Annonaceae	Evergreen
Scurrula chingii (Cheng) H. S. Kiu var. *yunnanensis*	Loranthaceae	Sc	*Millettia pulchra* (Benth.) Kurz	Mp	Fabaceae	Deciduous
			Combretum indicum (L.) Jongkind	Ci	Combretaceae	Deciduous
			Lagerstroemia indica L.	Li	Lythraceae	Deciduous
Viscum ovalifolium DC.	Santalaceae	Vo	*Millettia pulchra* (Benth.) Kurz	Mp	Fabaceae	Deciduous
			Balakata baccata (Roxb.) Esser	Bb	Euphorbiaceae	Evergreen

Nomenclature of plants follows iPlants (https://www.iplant.cn).

were conducted during the rainy season of 2023, from May to October, except leaf water potentials were measured during the dry season of 2024.

Functional traits

Hydraulic conductivity

Hydraulic conductivity was measured following the methodology by Sperry et al. (1988). The maximum vessel length (MVL) of branches was determined using the air injection method (Ewers and Fisher 1989). To minimize the influence of open vessels on hydraulic measurements, all sampled branches were ~1.5 times longer than the MVL. Six healthy branches were collected from three mature individuals of each mistletoe–host species pair before sunrise during the rainy season. These branches were wrapped in wet paper towels, sprayed with water, sealed in a black plastic bag and promptly transported to the laboratory. To prevent 'cutting under tension' artifacts (Wheeler et al. 2013, Torres-Ruiz et al. 2014), all bagged branches were cut 4–5 cm from the basal ends underwater and immersed in water for 1–2 h to release tension. After that, a stem segment 10% longer than the MVL was excised underwater. This target segment was flushed with a 10 mM potassium chloride solution (degassed ultrafiltrate) at a pressure of 100 kPa for ~30–60 min to remove native embolism. Subsequently, the segment was connected to a flow measurement apparatus with a head pressure of 2 kPa (equivalent to 20 cm of hydrostatic pressure) using a 10 mM degassed and filtered (0.2 μm) KCl solution. The distal end of the segment was connected to a pipette, and the flow F was calculated from the displacement of the meniscus inside the pipette once a steady flow rate was achieved. The maximum hydraulic conductivity (K_h) was then calculated using the following formula:

$$K_h = \frac{F \times L}{P} \quad (1)$$

where F is the mass flow rate (kg s^{-1}), P is the pressure gradient through the pipe section (MPa) and L is the length of the segment (m).

All leaves from each branch were collected, and the leaf areas (LAs) and cross-sections of the stem segments were scanned using a scanner (CanoScan, 9000F, Mark II, Thailand). The cross-section and LAs were then measured using ImageJ 1.54f (https://imagej.net/ij/) to determine the sapwood area (A_S) and leaf area (A_L). Sapwood-specific hydraulic conductivity (K_S; kg m^{-1} s^{-1} MPa^{-1}) and leaf-specific hydraulic conductivity (K_L; $\times 10^{-4}$ kg m^{-1} s^{-1} MPa^{-1}) were determined by dividing K_h by A_S and A_L, respectively. The HV (cm^2 m^{-2}) was calculated by dividing A_S by the A_L.

Stem xylem vulnerability curves

Vulnerability curves (VCs) of the stem xylem were generated using the bench-top dehydration method (Sperry et al. 1988, Chen et al. 2021). The same procedure for hydraulic conductivity measurements was followed for the collection and preparation of branches used in stem VCs. Under laboratory conditions, branches were subjected to varying levels of dehydration. Leaves from each branch were periodically sampled to measure water potential (Ψ_{leaf}; MPa) using a pressure chamber (PMS1505D-EXP, PMS Instrument Company, Corvallis, OR, USA). Once the target dehydration level was reached, the branches were enclosed in water vapor-saturated bags for $\geq$1 h to equilibrate water potential throughout. Two leaves (or terminal twigs) from different locations on each branch were then cut to verify the balance of Ψ_{leaf}. When the difference between two Ψ_{leaf} measurements was less than 0.3 MPa, their average was used to represent the xylem water potential. To prevent 'cutting under tension' artifacts, branches were cut underwater 30 cm from the base and soaked for 1 h to release tension until Ψ_{leaf} approached zero. A 10-cm segment was then cut underwater between 20 cm to 50 cm from the apex. The 10-cm segment was further trimmed at both ends with a sharp blade and connected to the hydraulic measurement system. The initial conductance (K_0) of the segment was determined as:

$$K_0 = \frac{F}{P} \quad (2)$$

where F is the water flux (kg s^{-1}) and P is the hydrostatic pressure (MPa).

After flushing the segment with a KCl solution at 100 kPa for 30–60 min, the maximum conductivity (K_{max}) was measured again. The percentage loss of conductivity (PLC) was calculated as:

$$PLC = 100 \times \frac{K_{max} - K_0}{K_{max}} \quad (3)$$

Table 2. Stem and leaf traits measured in this study.

	Trait	Code	Ecological significance	Unit
Stem traits	Xylem water potential at 12% loss of hydraulic conductivity	P_{12}	P_{12} reflects the initial embolisms (Urli et al. 2013)	MPa
	Xylem water potential at 50% loss of hydraulic conductivity	P_{50}	P_{50} reflects a plant's resistance to embolism (Haverroth et al. 2024)	MPa
	Xylem water potential at 88% loss of hydraulic conductivity	P_{88}	P_{88} reflects the critical point of irreversible xylem embolism (Urli et al. 2013)	MPa
	Sapwood-specific hydraulic conductivity	K_S	Related to xylem water transport efficiency (Mencuccini et al. 2019)	kg m^{-1} s^{-1} MPa^{-1}
	Sapwood density	WD	Related to mechanical resistance, and embolism resistance (Savi et al. 2019)	g cm^{-3}
	Vessel density	VD	Related to the water conductivity and mechanical safety (Chave et al. 2009)	no. mm^{-2}
	Hydraulically weighted vessel diameter	D_h	Related to water transport efficiency (Fu et al. 2012)	μm
Leaf traits	Leaf turgor loss point	TLP	Related to plant drought tolerance (Bartlett et al. 2012)	MPa
	Stomatal safety margin	HSM_{tlp}	Drought-avoiding species have a greater xylem safety margin (Skelton et al. 2015)	MPa
	Leaf-specific hydraulic conductivity	K_L	K_L reflects the hydraulic capacity of stem xylem to supply water to the leaves (Tyree and Zimmermann 2002)	$\times 10^{-4}$ kg m^{-1} s^{-1} MPa^{-1}
	Huber value	HV	HV indicates the water demand for maintaining per-unit leaf area (Mencuccini et al. 2019, van der Sande et al. 2019)	cm^2 m^{-2}
	Leaf water potentials during the dry season	Ψ_{mid}	Reflecting the minimum water potential during the dry season (Skelton et al. 2015)	MPa
	Leaf size	LS	Related to plant water-use strategies (Xu et al. 2019)	cm^2
	Specific leaf area	SLA	SLA indicates plant light-capturing capacity (Mencuccini et al. 2019)	cm^2 g^{-1}
	Leaf dry matter content	LDMC	Reflecting a plant's resource use and ecological adaptability (Blumenthal et al. 2020)	g g^{-1}
	Vein density	D_{vein}	Leaf vein density reflects leaf hydraulic efficiency (Brodribb and Jordan 2011)	mm mm^{-2}
	Stomatal density	SD	Related to carbon dioxide absorption and transpiration (Hetherington and Woodward 2003, Zweifel et al. 2012)	no. mm^{-2}
	Guard cell length	GCL	Larger guard cells and stomata result in large pores, enabling greater CO_2 assimilation (Hetherington and Woodward 2003)	μm
	Stomatal pore area index	SPI	SPI affects a plant's capacity for gas exchange and water regulation (Hetherington and Woodward 2003)	
	Stable carbon isotope composition	$\delta^{13}C$	Reflecting the long-term water use efficiency (Chen et al. 2013, Zhang et al. 2023)	‰
	Stable nitrogen isotope composition	$\delta^{15}N$	Identifying as an integrator of the N cycle and plant stress responses (Snyder et al. 2022)	‰

The VCs were then constructed using the PLC values and corresponding water potentials. A sigmoid function with three parameters was used to fit the VCs, based on PLC as a function of xylem tension (Ψ_0):

$$\mathrm{PLC} = \frac{100}{1 + \exp\left(a \times (\Psi_x - \Psi_0)\right)} \quad (4)$$

where a is the maximal slope of the curve and Ψ_0 is the stem water pressure causing 50% loss of conductivity (P_{50}). Additionally, the pressure that caused 12 (P_{12}) and 88% (P_{88}) loss of conductivity were calculated using Eq. (4).

Sapwood density and anatomy

After measuring the hydraulic conductivity, a 5-cm segment was cut from the base of the branch. The bark and pith were removed, and the segment was soaked in water for 12 h to achieve saturation. The fresh volume of the wood was determined using the water displacement method. The sample was then dried in an oven at 80 °C for 72 h. The dry weight of the sample was measured using a balance with an accuracy of 0.0001 g (Mettler Toledo, AL204, Shanghai, China). Sapwood density (WD; g cm^{-3}) was calculated as the ratio of dry weight to fresh volume. Additional wood samples were fixed in FAA solution (900 mL 70% ethanol, 50 mL formalin and 50 mL of 17.5 mol L^{-1} glacial acetic acid) for anatomical measurements.

Wood anatomy was examined using paraffin-embedded tissue sectioning. The samples were dehydrated in a series of ethanol solutions (50, 70, 80, 95 and 100%) and D-limonene, followed by immersion in liquid paraffin, and then embedded in paraffin blocks (Rossi et al. 2006). Sections, 14–25 μm thick, were cut from the paraffin blocks using a rotary microtome (Leica Microsystems Ltd, Leica DM2500, Wetzlar, Germany). The sections were stained with 1% Safranin-O for 2–3 h and then with 0.5% Astra Blue for 2 min, and mounted with neutral gum (Moser et al. 2010). Images were captured using a light microscope (Leica Microsystems Ltd, Leica DM2500, Wetzlar, Germany) and analyzed with ImageJ 1.54f.

The diameter (D) of each vessel (i) was calculated using the equation of (Meunier et al. 2020):

$$D_i = 2\sqrt{\frac{A_i}{\pi}} \quad (5)$$

where A_i (μm^2) represents the area of vessel i, and π is ~3.14.

The hydraulically weighted vessel diameter (D_h; μm) of each individual was calculated according to Sterck et al. (2008):

$$D_h = \left[\left(\frac{1}{n}\right)\sum_{i=1}^{n} {D_i}^4\right]^{\frac{1}{4}} \quad (6)$$

Vessel density (VD; no. mm^{-2}) was determined by counting the number of vessels per unit area.

Water potential at turgor loss point

Water potential at turgor loss point (TLP; MPa) was assessed following the method of Bartlett et al. (2012), using measurements of leaf osmotic potential at full turgor (Ψ_{osm}; MPa). To ensure accurate measurement, branches with healthy mature leaves were rehydrated overnight. Before measurement, two leaves from each branch segment were stored in humidified plastic bags to prevent dehydration. For each leaf, one 8-mm diameter disc was punched out, carefully avoiding the major vein. Each disc was then wrapped in aluminum foil and submerged in liquid nitrogen for 2 min. After liquid nitrogen treatment, the frozen discs were quickly punctured at least 15 times using sharp-tipped tweezers and placed in an osmotic chamber within 30 s. The Ψ_{osm} was then determined using a vapor pressure osmometer chamber at 25 °C (WESCOR Co., VAPRO 5600, Logan, UT, USA). Turgor loss point was then calculated by converting the measured values of Ψ_{osm} to TLP using the equation proposed by Bartlett et al. (2012). The hydraulic safety margin (HSM_{tlp}) was calculated as the difference between TLP and P_{50} (Skelton et al. 2021). To assess season water potential variation, we measured midday leaf water potentials during the dry season (Ψ_{mid}; MPa) for both mistletoes and their hosts. Measurements were conducted at the peak of the dry season (in March 2024), using the pressure chamber (PMS1505D-EXP, PMS Instrument Company, Corvallis, OR, USA).

Leaf morphology

For each species pair, three individuals were selected, and 8–12 leaves from each individual were used to measure the LA using a scanner. For the compound leaf, all leaflets from each compound leaf were included. LA (cm^2) was measured with the ImageJ 1.54f. The leaves were then soaked in water for 12 h, and after wiping off the leaf surface moisture, the saturated weight was immediately measured using a balance (Mettler Toledo, AL204, Shanghai, China). Finally, the leaves were dried in an oven at 80 °C for 48 h to obtain the dry weight. LDMC (g g^{-1}) was calculated as the ratio of dry weight to saturated weight, and the SLA (cm^2 g^{-1}) was calculated as the ratio of LA to dry weight.

Leaf anatomy

We used the nail polish imprint method to measure stomatal traits on three leaves from each of the three individuals per species. Since mistletoes have stomata on both leaf epidermis, stomatal imprints were made on both the upper and lower epidermis of mistletoe leaves and the lower epidermis of the host plant leaves. Images at ×200 and ×400 magnifications were acquired with a light microscope (Leica Microsystems Ltd, Leica DM2500, Wetzlar, Germany). The guard cell length (GCL; μm) and stomatal density (SD; no. mm^{-2}) were measured using the ImageJ 1.54f. SD for the host was calculated as the number of stomata per unit area. For mistletoes, SD was calculated as the sum of the densities on the upper and lower epidermis, while GCL was averaged between the two epidermis. The stomatal pore area index (SPI) was calculated as SD × GCL^2. For leaf vein density, 1-cm^2 leaf segments avoiding the midrib, were selected and boiled in 5% NaOH solution for 3–4 h. After bleaching, the samples were stained with 1% Safranin-O. Images were captured with a light microscope (Leica Microsystems Ltd, Leica DM2500, Wetzlar, Germany), with at least 30–36 images taken for each species. Vein density (D_{vein}; mm mm^{-2}) was calculated as the total vein length per LA.

Leaf nutrient concentrations and stable isotope

Fresh leaf samples were oven-dried at 80 °C for at least 48 h. The dried samples were then ground and sequentially passed through a 100-mesh sieve to prepare for further analysis.

Leaf powder samples were sent to the Stable Isotope Laboratory of Shenzhen Huake Precision Testing Inc., Shenzhen, China, to analyze the $\delta^{13}C$ and $\delta^{15}N$. These measurements were conducted using an elemental analyzer (Thermo Fisher Scientific Inc., Flash 2000HT, Waltham, MA, USA) coupled with an isotope ratio mass spectrometer (Thermo Fisher Scientific, Finnigan Delta V Advantage). Stable isotope ratios were expressed in δ-unit notation and calculated using the following formula:

$$\delta X = \left[\left(\frac{R_{sample}}{R_{standard}}\right) - 1\right] \times 1000‰ \quad (7)$$

where X is ^{13}C or ^{15}N and R_{sample} is the $^{13}C/^{12}C$ ratio for carbon or the $^{15}N/^{14}N$ ratio for N.

Statistical analyses

All statistical analyses and visualizations were conducted using R version 4.3.3 (R Core Team 2024). To improve the assumptions of residual normality and homogeneity of variance, all data were log-transformed prior to analysis. Negative values of P_{12}, P_{50}, P_{88}, TLP and $\delta^{13}C$ were converted to positive values, and $\delta^{15}N$ were uniformly adjusted by adding 1 before transformation. Data normality was assessed using the Shapiro–Wilk test, and homogeneity of variances was evaluated with the Bartlett test. Except for the linear mixed-effects models (LMMs) based on individual-level data, all other analyses were conducted at the species-pair level data.

The LMMs were employed to evaluate whether the measured traits differed between life forms (mistletoe *vs* host). In these models, P_{12}, P_{50}, P_{88}, K_S, WD, VD, D_h, TLP, HSM_{tlp}, K_L, HV, Ψ_{mid}, LS, SLA, LDMC, D_{vein}, SD, GCL, SPI, $\delta^{13}C$ and $\delta^{15}N$ were treated as dependent variables. Life form was a fixed factor with two levels (mistletoe or host), while species pair was treated as a random effect to account for both the repeated measurements from the same plants and the non-independence of mistletoe species across different species pairs. The LMMs were fitted using the *lmer* function of the 'lme4' package (Bates et al. 2015). A paired-samples *t*-test was conducted to evaluate differences in functional traits for each mistletoe–host species pair, except for P_{12}, P_{50} and P_{88}, utilizing the *t.test* function from the 'stats' package. Vulnerability curves for each mistletoe–host species pair were constructed using the *fitplc* function of the 'fitplc' package (Duursma and Choat 2017). Confidence intervals (CI) for P_{12}, P_{50} and P_{88} were calculated, and the differences in embolism resistance among species were then evaluated based on these CIs (Duursma and Choat 2017). To explore whether mistletoe species exhibited significant differences in hydraulic traits based on their host species, we performed separate analyses for the three mistletoe species, using host species as a predictive factor in Analysis of Variance (ANOVA). When the ANOVA results were significant, we conducted post-hoc pairwise comparisons.

Pearson's correlations were employed to examine the relationships between traits, using the *cor_test* function in R. To assess whether the correlation between traits (e.g., TLP and SPI) in mistletoes is driven by intraspecific variation (difference within the same mistletoe species across different host species) or interspecific variation (differences between different mistletoe species), we used LMMs to partition the variance into components corresponding to intraspecific and interspecific effects. Specifically, the fixed effect was the correlation between the traits, while the random effect was mistletoe species. We then used the *VarCorr* function from the 'lme4' package to extract the model's variance components and calculated the relative contribution of interspecific variation (explained by mistletoe species as a random effect) and intraspecific variation (captured by the residual variance in the model). Standardized major axis regressions were fitted using the *sma* function of the 'smart package' (Warton et al. 2012) to compare bivariate relationships between life forms. Principal component analysis (PCA) was conducted using the *PCA* function in the 'FactoMineR' package (Lê et al. 2008) to determine whether mistletoes and hosts occupied different multivariate trait spaces. The *adonis2* function from the 'vegan' package (Kotowska et al. 2015) was used to perform a Permutational Multivariate Analysis of Variance (PERMANOVA) to test whether mistletoes and hosts could be distinguished in the multi-dimensional trait space.

Results

Differences in stem and leaf functional traits between mistletoes and hosts

Mistletoes had significantly more negative P_{12} value (xylem water potential at 12% loss of hydraulic conductivity), higher sapwood density (WD) and vessel density (VD) compared with their host plants ($P < 0.05$; Figure 1a, e and f; see Table S1 available as Supplementary Data at *Tree Physiology* Online). In contrast, their sapwood-specific hydraulic conductivity (K_S) and hydraulically weighted vessel diameter (D_h) were significantly lower than those of their hosts ($P < 0.001$; Figure 1d and g). Overall, no significant differences were observed in the xylem water potential at 50 and 88% loss of hydraulic conductivity (P_{50} and P_{88}, respectively) between mistletoes and their hosts ($P > 0.05$; Figure 1b and c). The P_{50} of mistletoes ranged from −2.93 to −5.20 MPa (−4.01 ± 0.31 MPa on average), while that of the hosts ranged from −2.43 to −6.36 MPa (−3.95 ± 0.40 MPa on average). Specifically, in two species pairs, *D. pentandra-Monoon similarum* (Dp-Ms) and *S. chingii* var. *yunnanensis-Lagerstroemia indica* (Sc-Li), mistletoes showed a lower embolism resistance than their hosts, displaying less negative P_{50} values (Figure 2c and f, see Table S2 available as Supplementary Data at *Tree Physiology* Online). However, no significant differences were found in the remaining six species pairs. In five species pairs, Dp-Ec, Dp-Mpa, Sc-Ci, Vo-Mp and Vo-Bb, mistletoes had slightly more negative P_{50} values compared with their hosts, although these differences were not statistically significant, as indicated by overlapping CI (see Figure 2a, b, e, g and h).

Mistletoes exhibited significantly more negative TLP, midday leaf water potentials during the dry season (Ψ_{mid}), higher HV, GCL, compared with their host plants ($P < 0.05$; Figure 3a, e, d and k, see Table S1 available as Supplementary Data at *Tree Physiology* Online). In contrast, mistletoes displayed significantly lower leaf size (LS), SLA, LDMC, vein density (D_{vein}), SD, leaf-specific hydraulic conductivity (K_L) and stable carbon isotope composition ($\delta^{13}C$), than host plants ($P < 0.05$; Figure 3c, f–j, and m). The TLP of mistletoes ranged from −1.81 to −2.48 MPa (−2.05 ± 0.08 MPa on average), while that of the hosts ranged from −1.53 to −2.46 MPa (−1.93 ± 0.10 MPa on average). However, no significant differences were observed in the stomatal safety

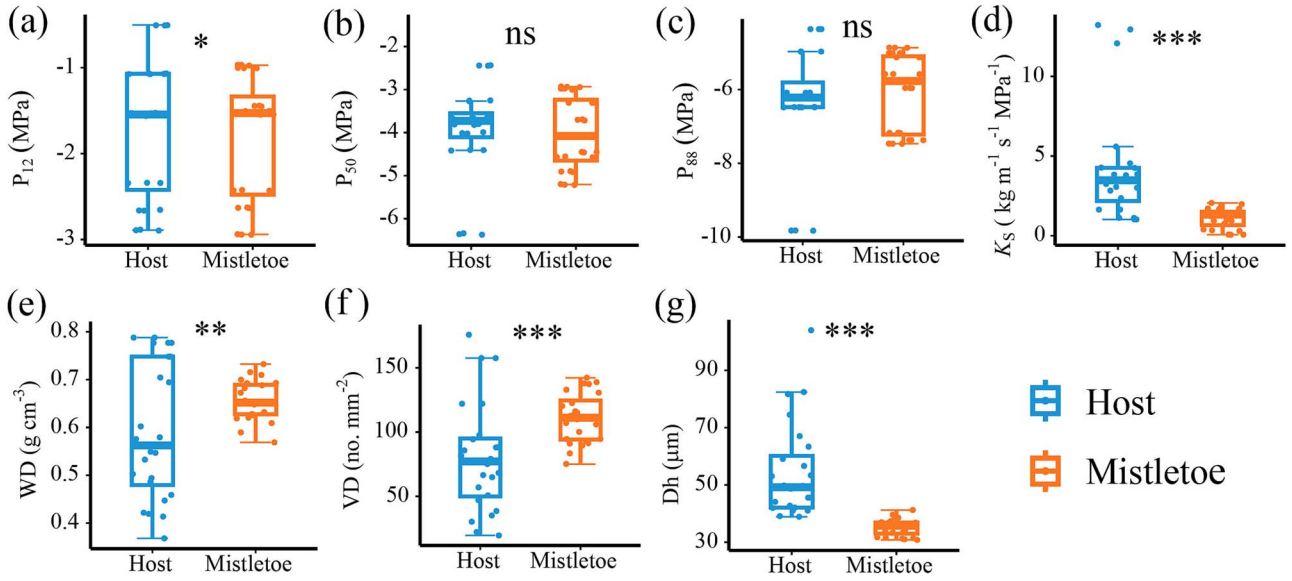

Figure 1. Box plot showing the differences in stem functional traits between mistletoes and host plants. (a) Xylem water potential at 12% loss of hydraulic conductivity (P_{12}); (b) xylem water potential at 50% loss of hydraulic conductivity (P_{50}); (c) xylem water potential at 88% loss of hydraulic conductivity (P_{88}); (d) sapwood-specific hydraulic conductivity (K_S); (e) sapwood density (WD); (f) vessel density (VD); (g) hydraulically weighted mean vessel diameter (D_h). ns, $P > 0.05$; $^*P < 0.05$; $^{**}P < 0.01$; $^{***}P < 0.001$.

margin (HSM_{tlp}), SPI and stable nitrogen isotope composition ($\delta^{15}N$) between mistletoes and host plants ($P > 0.05$; Figure 3b, l and n). Additionally, the random effect of species pair had a significant influence on the comparison of stem and leaf functional traits between mistletoes and hosts (see Table S3 available as Supplementary Data at *Tree Physiology* Online).

Notably, we found that P_{12}, P_{50} and P_{88} values significantly differed for each of three mistletoe species growing on different host species (see Table S4 available as Supplementary Data at *Tree Physiology* Online). In addition, other drought-related traits, such as HSM_{tlp}, WD, Ψ_{mid}, LS, $\delta^{13}C$, TLP and HV, also showed significant differences (see Table S4 available as Supplementary Data at *Tree Physiology* Online).

Associations among stem and leaf functional traits

P_{50} was not significantly correlated with either K_S or WD in both mistletoes and hosts (Figure 4a and b; see Tables S5 and S6 available as Supplementary Data at *Tree Physiology* Online). In contrast, K_S showed a positive correlation with D_h in mistletoes, and a positive correlation with Ψ_{mid} in hosts (Figure 4c and d).

In mistletoes, TLP showed a positive correlation with HV and GCL, and a negative correlation with LS and SD (Figure 5a–d; see Tables S5 and S6 available as Supplementary Data at *Tree Physiology* Online). Moreover, in mistletoes, LDMC was negatively correlated with SLA and D_{vein} (Figure 5e and f), while SD was negatively correlated with GCL but positively correlated with D_{vein} (Figure 5g and h). In contrast, D_{vein} was negatively associated with GCL in both mistletoes and hosts, sharing a common slope; however, hosts displayed a higher intercept (Figure 5i; see Tables S5–S7 available as Supplementary data at *Tree Physiology* Online).

P_{50} was positively correlated with HSM_{tlp} in both mistletoes and hosts, exhibiting a common slope and intercept (Figure 6a; see Tables S5–S7 available as Supplementary data at *Tree Physiology* Online). Although P_{50} in both mistletoes and hosts showed a positive correlation with LDMC with a common slope, mistletoes showed a higher intercept (Figure 6b). In mistletoes, P_{50} was negatively linked with SLA and D_{vein} (Figure 6c and d; see Tables S5 and S6 available as Supplementary data at *Tree Physiology* Online). No significant correlation was found between P_{50} and TLP in either mistletoes or hosts (Figure 6e). In contrast, K_S was negatively related to TLP and HV only in mistletoes (Figure 6f and g). K_S showed a positive correlation with SD in both mistletoes and hosts, with a common slope but hosts showing a higher intercept (Figure 6h; see Tables S5–S7 available as Supplementary data at *Tree Physiology* Online). Additionally, SD was positively correlated with D_h exclusively in mistletoes (Figure 6i; see Tables S5 and S6 available as Supplementary data at *Tree Physiology* Online).

In addition, the trait correlations in mistletoes were driven by both intraspecific variation (i.e., plastic responses to different hosts) and inherent interspecific differences (i.e., across mistletoe species). However, interspecific variation played a more important role because different species in most figures are clearly separated, and interspecific trait variation contributed more to the variance in trait correlations (Figures 4–6; see Table S8 available as Supplementary data at *Tree Physiology* Online).

Trait differences between mistletoes and hosts in multivariate space

The *PCA* results of 7 stem traits and 14 leaf traits from eight mistletoe–host species pairs revealed that the first and second principal components accounted for 35.4 and 23% of the total variance, respectively (Figure 7). The first axis was positively correlated with K_L, K_S, D_h, SLA, D_{vein} and SD, and negatively associated with $\delta^{13}C$, VD, GCL and TLP (Figure 7a; see Table S9 available as Supplementary data at *Tree Physiology* Online). The second axis was positively correlated with traits indicative of drought resistance, such as P_{12}, P_{50}, P_{88}, HSM_{tlp}, LS and LDMC, and negatively associated with HV,

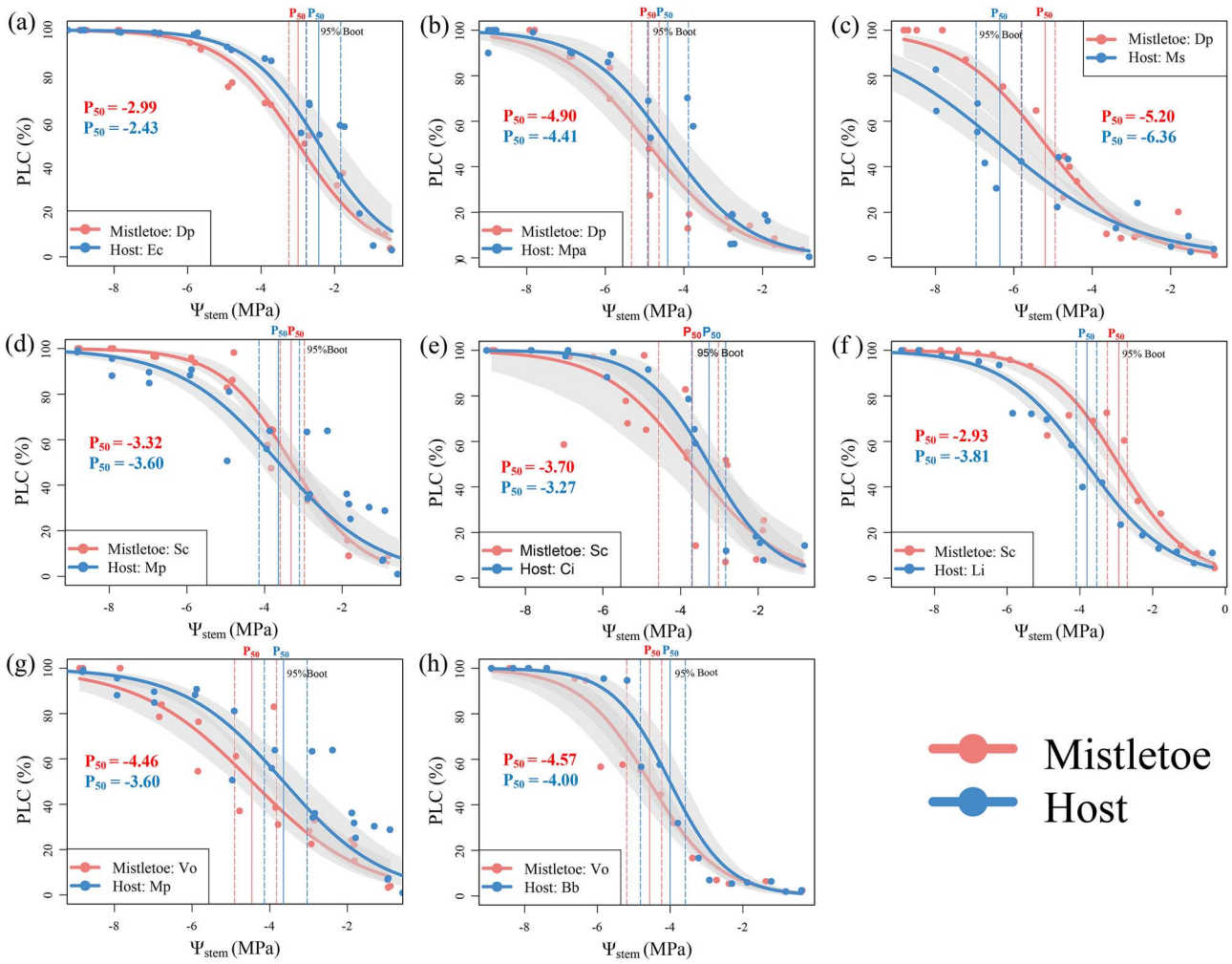

Figure 2. Vulnerability curves for eight mistletoe–host species pairs. The percentage loss of conductivity (PLC) correlates with xylem water potential across various species pairs: (a) *Dendrophthoe pentandra* and *Elaeagnus conferta* (Dp-Ec); (b) *Dendrophthoe pentandra* and *Microcos paniculata* (Dp-Mpa); (c) *Dendrophthoe pentandra* and *Monoon simiarum* (Dp-Ms); (d) *Scurrula chingii* var. *yunnanensis* and *Millettia pulchra* (Sc-Mp); (e) *Scurrula chingii* var. *yunnanensis* and *Combretum indicum* (Sc-Ci); (f) *Scurrula chingii* var. *yunnanensis* and *Lagerstroemia indica* (Sc-Li); (g) *Viscum ovalifolium* and *Millettia pulchra* (Vo-Mp); (h) *V. ovalifolium* and *Balakata baccata* (Vo-Bb). Solid lines denote P_{50} values (the water potential at which 50% loss of hydraulic conductivity), whereas dashed lines indicate 95% CI for these P_{50} values.

and WD (Figure 7a; see Table S9 available as Supplementary data at *Tree Physiology* Online). Mistletoes and hosts were separated along the first axis, with mistletoes showing lower branch hydraulic conductivity and reduced leaf water use efficiency, while hosts exhibited opposing traits (Figure 7b; see Table S10 available as Supplementary data at *Tree Physiology* Online).

Discussion

To the best of our knowledge, this study represents the first comprehensive comparison of hydraulics and drought resistance related stem and leaf functional traits between mistletoes and their hosts, incorporating a suite of morphological, anatomical and hydraulic traits, particularly involving the first direct measurements of mistletoe embolism resistance. Our results reveal distinct hydraulic strategies between mistletoes and their hosts. Specifically, mistletoes displayed more drought tolerance traits compared with their hosts, and were able to withstand lower water potentials during the dry season. Interestingly, both mistletoes and their hosts showed high resistance to drought-induced embolism (with average P_{50} values around −4 MPa), which could be because the study site has a distinct dry season.

Mistletoes employ a more drought resistant strategy than their hosts, despite their higher water use

Consistent with our first hypothesis, mistletoes are more drought tolerant than their hosts, characterized by more negative Ψ_{mid}, P_{12} and TLP values, higher WD and VD, and lower LS and SLA. Meanwhile, they show lower hydraulic efficiency, as indicated by D_{vein}, K_L, K_S and D_h (Figure 1a and d–g; Figure 3a, c, e, f and h; see Table S1 available as Supplementary data at *Tree Physiology* Online), which is in line with the findings of a recent study based on xylem anatomy (Zhang et al. 2025). Previous studies have demonstrated that mistletoes must tolerate lower leaf water potentials than their hosts (He et al. 2021, Ye et al. 2021), which necessitates high embolism resistance (Nardini et al. 2011, Jin et al. 2023). Given that HV, D_h, WD and VD are associated with embolism resistance (Fu et al. 2012, Savi et al. 2019,

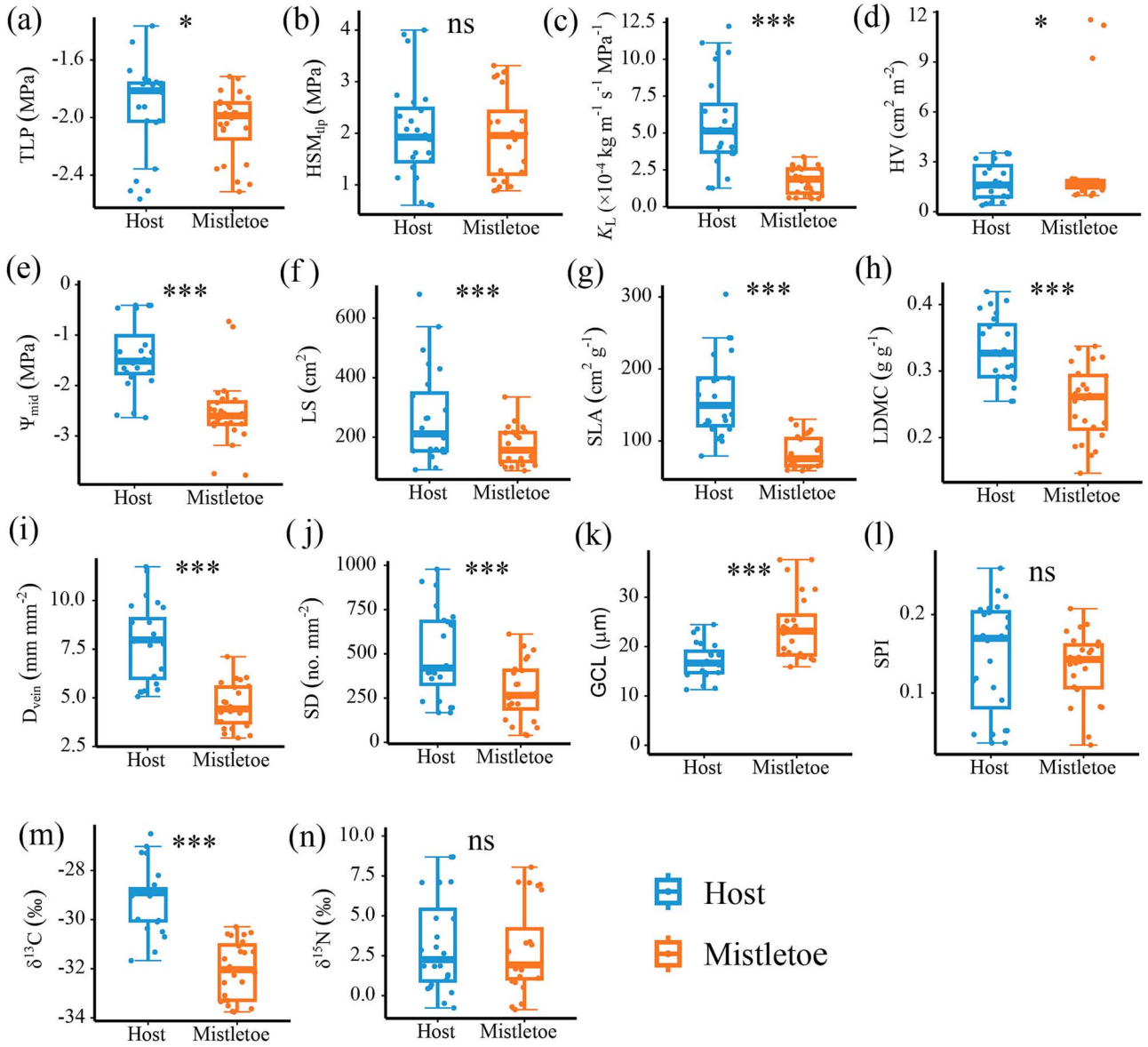

Figure 3. Box plot illustrating variations in leaf functional traits between mistletoes and host plants. (a) Leaf TLP; (b) HSM_{tlp}; (c) leaf-specific hydraulic conductivity (K_L); (d) HV; (e) leaf water potentials during the dry season (Ψ_{mid}); (f) LS; (g) SLA; (h) LDMC; (i) vein density (D_{vein}); (j) SD; (k) GCL; (l) SPI; (m) stable carbon isotope composition ($\delta^{13}C$); (n) stable nitrogen isotope composition ($\delta^{15}N$). ns, $P > 0.05$; *$P < 0.05$; ***$P < 0.001$.

Liang et al. 2021), this set of features, i.e., lower D_h and K_S, coupled with higher HV, WD and VD, help mistletoes to counteract the risks of embolism resulting from high xylem tension (lower leaf water potential and relatively high VPD in the upper canopy). Here, the more negative Ψ_{mid} values in mistletoes than in their hosts provide further evidence supporting the hypothesis that mistletoes maintain lower water potentials than their hosts to sustain a continuous water flux. The ability of mistletoes to tolerate lower water potentials suggests a high degree of drought resistance. Furthermore, the more negative P_{12} values indicate a later embolism initiation in mistletoes, highlighting the importance for them to maintain hydraulic safety in a daily basis. The lack of significant differences in P_{50} between mistletoes and hosts was probably due to convergent adaptation of both mistletoes and hosts to seasonal drought in the study site (Figure 1b; see Table S1 available as Supplementary data at *Tree Physiology* Online). Indeed, both groups showed rather negative P_{50} values close to −4 MPa. In addition, high interspecific variation was found. Specifically, in the Dp-Ms and Sc-Li parasite–host pairs, mistletoes had lower embolism resistance than their hosts (Figure 2c and f). In contrast, mistletoes had more negative P_{50} values than their hosts in five species pairs, despite being non-significant (Figure 2a, b, e, g and h). Additionally, the LMMs, with mistletoe–host species pair as a random effect, revealed a significant influence of species pair on the observed trait differences between mistletoes and their hosts. Overall, these findings suggest that species specificity should be considered when analyzing trait differences between mistletoes and hosts. To our knowledge, this is the first evaluation of embolism resistance (P_{50}) in mistletoes, and future studies could further clarify these differences by increasing the sample size in terms of both mistletoe species and species pairs.

We found that mistletoes have lower water use efficiency than their hosts (Figure 3m; see Table S1 available as Supplementary data at *Tree Physiology* Online), consistent

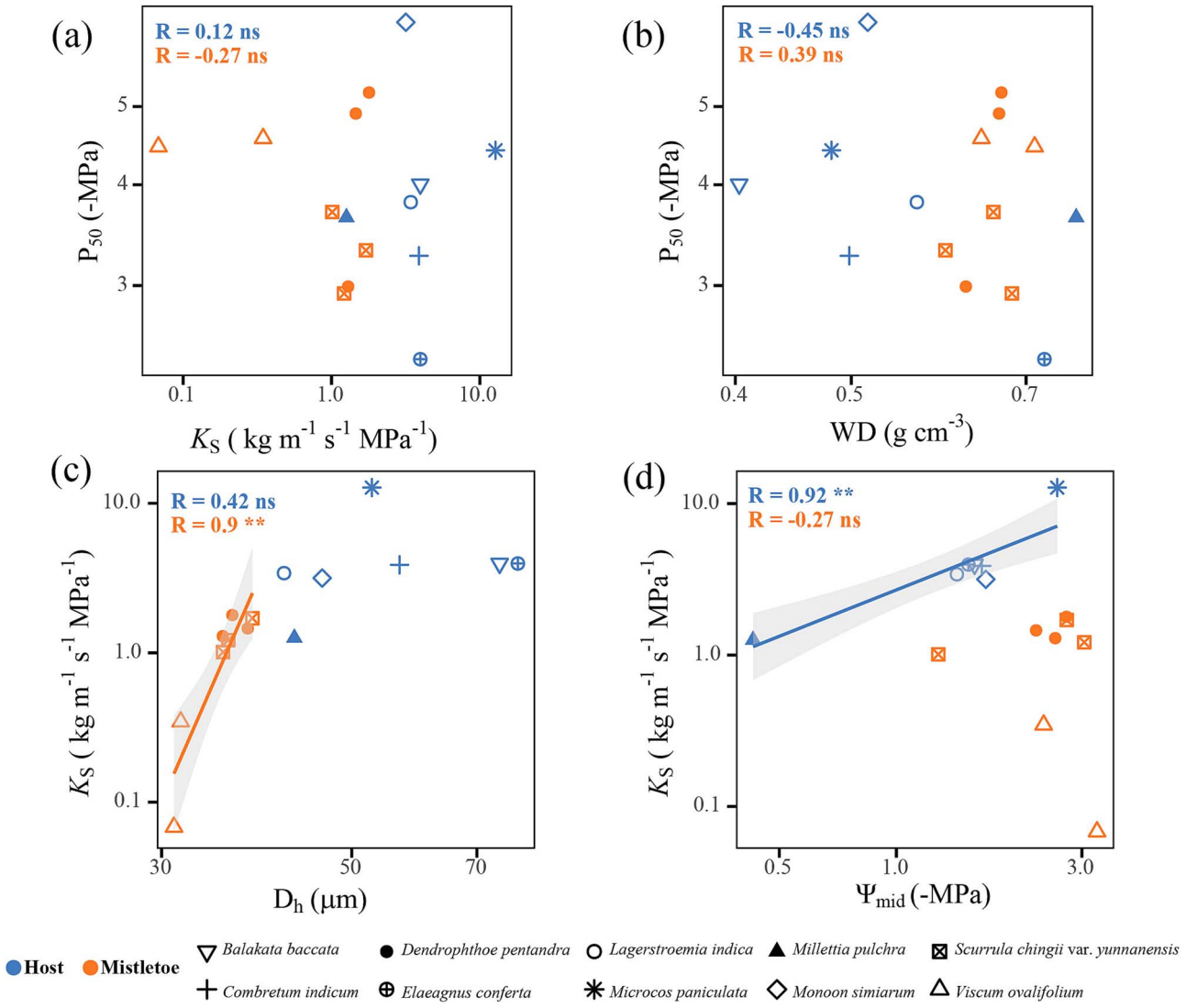

Figure 4. Correlations among functional traits in mistletoes and hosts. Correlations displayed are: (a) xylem water potential at 50% loss of hydraulic conductivity (P_{50}) and sapwood-specific hydraulic conductivity (K_S), (b) P_{50} and sapwood density (WD), (c) K_S and hydraulically weighted mean vessel diameter (D_h) and (d) K_S and leaf water potentials during the dry season (Ψ_{mid}). Regression lines are given only when bivariate correlations are significant. ns, $P > 0.05$; $^{**}P < 0.01$.

with the results of previous studies (Chen et al. 2013, Zhang et al. 2023). This suggests that mistletoes adopt a profligate water use strategy despite relatively low hydraulic efficiency. Previous studies have consistently proven that mistletoes exhibit higher stomatal conductance and transpiration rates than their hosts (Zweifel et al. 2012, Griebel et al. 2022). However, we observed that mistletoes possess lower K_S, K_L and D_{vein} (proxy of leaf water supply efficiency) than their hosts, indicating lower water supply capacity, which contradicts their higher water use demands. Further, mistletoes also displayed lower stomatal densities and larger GCLs. Previous studies have shown that smaller stomata are associated with more sensitive stomatal closure, whereas lower stomatal densities and larger stomata are associated with slower physiological adjustments in stomatal conductance (Hetherington and Woodward 2003, Lawson and Blatt 2014, Haverroth et al. 2024). These observations suggest that mistletoes in our study possess structural features associated with weak stomatal regulation, aligning with earlier findings (Urban et al. 2012, Zweifel et al. 2012).

The ability of mistletoes to maintain higher stomatal conductance and transpiration rates may be attributed to several other traits. Lower SLA and LDMC in mistletoes, consistent with previous studies (Richards et al. 2021, Zhang et al. 2023), suggest that mistletoes have fleshy and succulent leaves that enhance water storage capacity. Furthermore, more negative TLP values in mistletoes compared with their hosts may facilitate higher stomatal conductance at lower leaf water potentials, as demonstrated in non-parasitic plants (Bartlett et al. 2012). These mechanisms mentioned above allow mistletoes to rehydrate before their hosts, prolonging stomatal openness (Carter and White 2009). Taken together, mistletoes adopt distinct ecological strategies characterized by a combination of traits that support their parasitic lifestyle.

Surprisingly, our results provide compelling evidence of the significant plasticity of mistletoe hydraulic traits in response to their host species. Specifically, we observed that key hydraulic traits, including P_{12}, P_{50} and P_{88}, varied significantly across different host species for each mistletoe species, indicating that mistletoes are able to adjust their

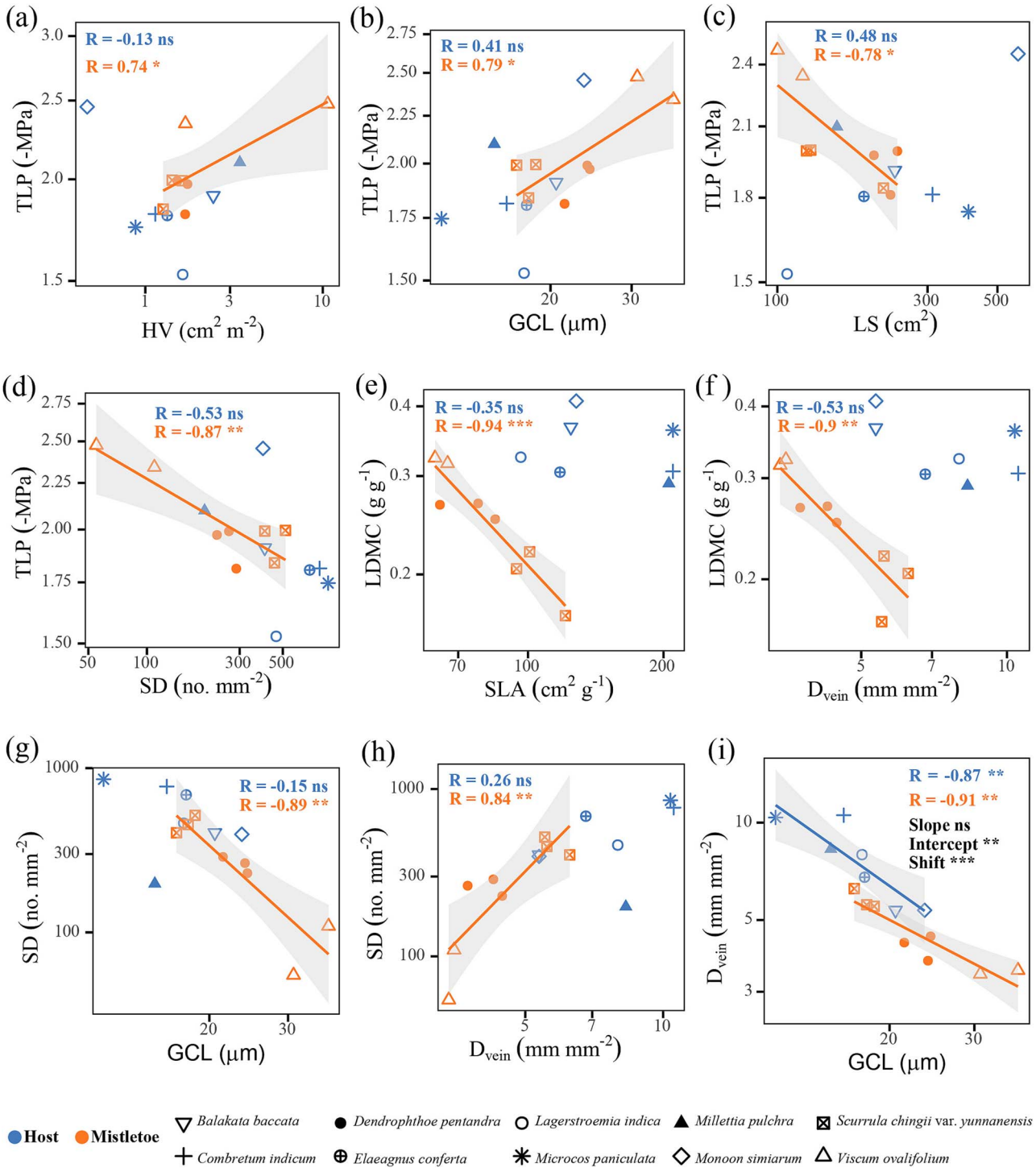

Figure 5. Correlations among leaf hydraulic and economic traits in mistletoes and hosts. Correlations displayed are: (a) leaf TLP with HV, (b) TLP with GCL, (c) TLP with LS, (d) TLP with SD, (e) SLA with LDMC, (f) LDMC with vein density (D_{vein}), (g) SD with GCL, (h) SD with D_{vein} and (i) D_{vein} with GCL. Regression lines are given only when bivariate correlations are statistically significant. If the trait relationship was significant for both mistletoes and host plants, the slope, intercept and shift were tested using standard major axis analysis (SMA). ns, $P > 0.05$; $^{*}P < 0.05$; $^{**}P < 0.01$; $^{***}P < 0.001$.

hydraulic vulnerability according to the characteristics of their host species. Notably, while previous studies have shown that embolism resistance, as indicated by P_{50}, tends to exhibit limited plasticity (Lamy et al. 2014, Lobo et al. 2018), our findings indicate that mistletoe embolism resistance is highly plastic in relation to their host species. This suggests that mistletoes may possess a greater degree of hydraulic flexibility than previously thought. Similar plasticity in embolism resistance has been observed in other species, such as *Fagus sylvatic* L., where embolism resistance varies across different populations (Wortemann et al. 2011, Skelton et al. 2019).

The differences in hydraulic traits were not limited to embolism resistance but extended to other drought tolerance-related traits, such as HSM_{tlp}, WD, Ψ_{mid}, LS, $\delta^{13}C$, TLP, and

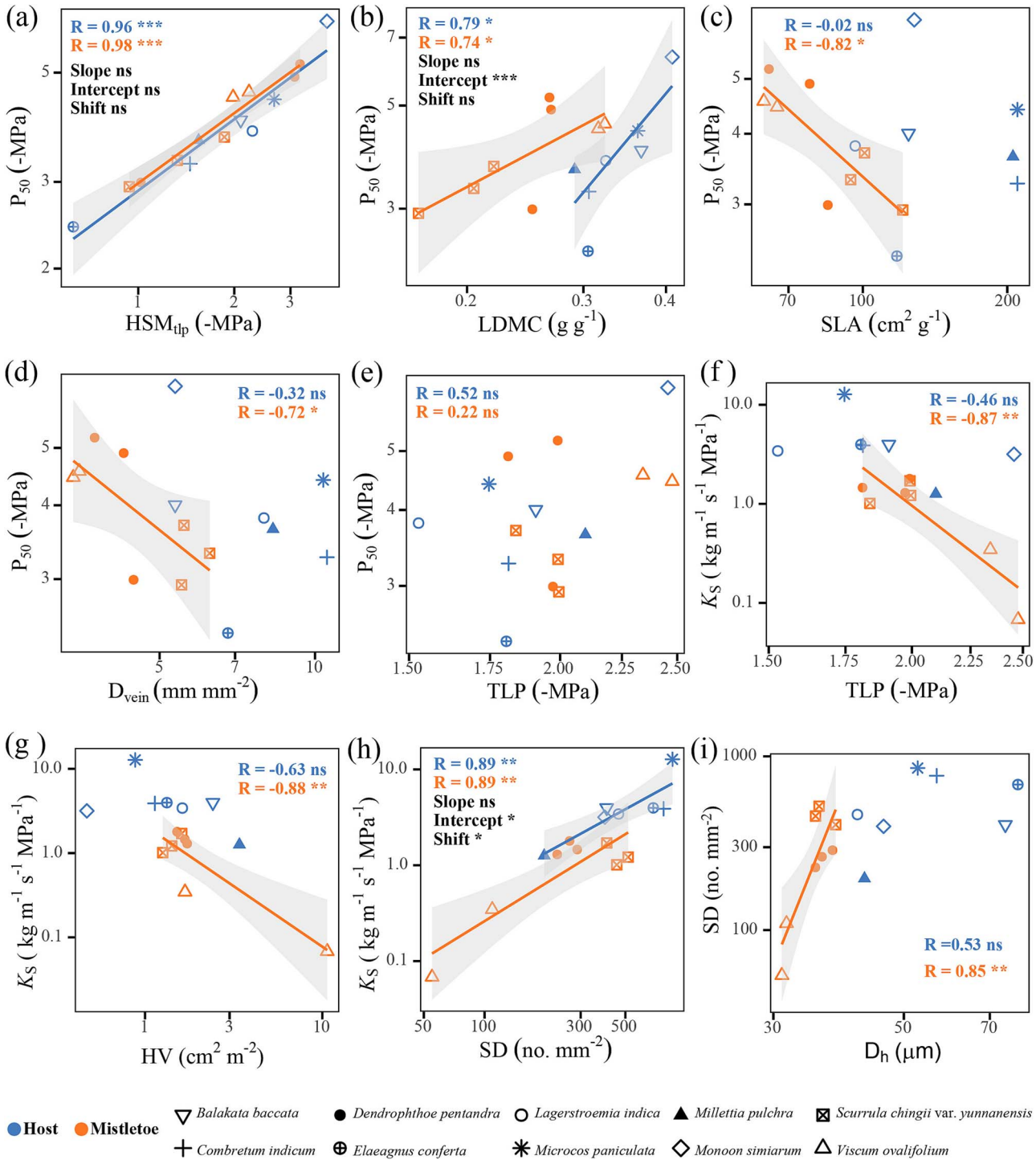

Figure 6. Correlations between stem and leaf functional traits in mistletoes and hosts. Correlations displayed are: (a) xylem water potential at 50% loss of hydraulic conductivity (P_{50}) and hydraulic safety margin (HSM_{tlp}), (b) P_{50} and LDMC, (c) P_{50} and SLA, (d) P_{50} and vein density (D_{vein}); (e) P_{50} and leaf TLP, (f) sapwood-specific hydraulic conductivity (K_S) and TLP, (g) K_S and HV, (h) K_S and SD and (i) SD and hydraulically weighted mean vessel diameter (D_h). Regression lines are given only when bivariate correlations are statistically significant. If the trait relationship was significant for both mistletoes and host plants, the slope, intercept and shift were tested using standard major axis analysis (SMA). ns, $P > 0.05$; $^*P < 0.05$; $^{**}P < 0.01$; $^{***}P < 0.001$.

HV. These findings further suggest that mistletoes exhibit a considerable degree of physiological flexibility, potentially driven by the hydraulic properties of the host. These results align with our previous research, which shows that host characteristics can drive physiological, morphological and hydraulic adjustments in mistletoes (Zhang et al. 2023, 2025). The ability of mistletoes to adjust their hydraulic traits may confer an adaptive advantage, enabling mistletoes to thrive in a variety of ecological niches and cope with environmental variability.

Trait coordination between mistletoes and their hosts

No significant correlation was observed between P_{50} and K_S or WD either across mistletoes or their hosts (Figure 4a and b;

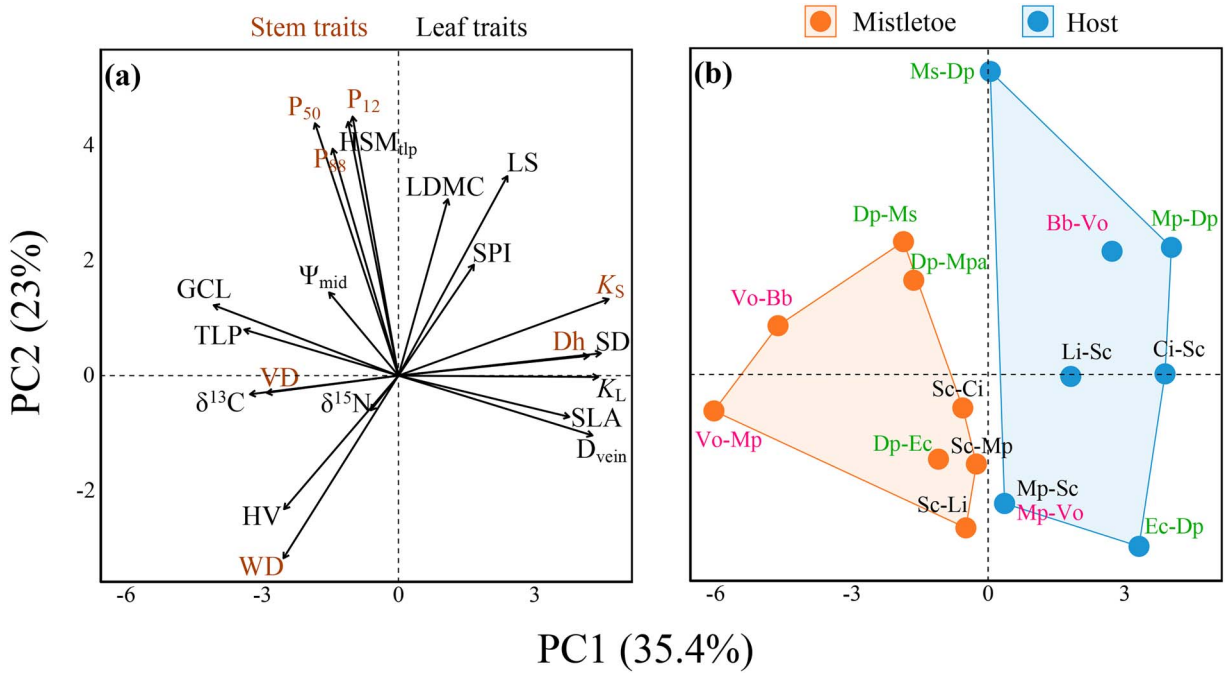

Figure 7. Biplot illustrating the first two axes of the PCA for the 21 functional traits (a), along with the loadings of eight mistletoe–host species pairs (b). All variables were log-transformed prior to analysis. Units for $\delta^{13}C$ are specified as (−‰), for $\delta^{15}N$ as (‰) and for hydraulic variables (P_{12}, P_{50}, P_{88}, Ψ_{mid} and TLP) as (−MPa). See Table 2 for trait abbreviations.

see Tables S5 and S6 available as Supplementary data at *Tree Physiology* Online). This indicates an overall lack of trade-off between hydraulic efficiency and safety, which contradicts our second hypothesis. These results are contrary to previous findings (van der Sande et al. 2019, Liu et al. 2024, Zhang et al. 2024), but in line with other studies (Zhu et al. 2013, Zhang et al. 2019). Indeed, the hydraulic efficiency-safety trade-off is species- and environment-dependent (Gleason et al. 2016, Liu et al. 2021). The absence of a trade-off between K_S and P_{50} in our study is likely due to the following reasons. Firstly, the observed trait correlations within mistletoes are driven by both intraspecific variation (i.e., plastic responses to different hosts) and inherent interspecific difference (Figure 4; see Table S8 available as Supplementary data at *Tree Physiology* Online). In non-parasitic plants, studies have shown that intraspecific trait correlations can sometimes decouple or even exhibit patterns opposite to those observed at the interspecific level (Anderegg et al. 2018, Fajardo et al. 2022). This may explain the decoupled relationship in mistletoes, with intraspecific variation dominating the correlation between K_S and P_{50}. Secondly, it could be because of functional adjustments in xylem tissue organization and intervessel pit structure in mistletoes. For instance, the spatial arrangement of xylem parenchyma can be associated with high K_S for a given P_{50} (Aritsara et al. 2023); P_{50} is strongly linked to intervessel pit membrane thickness (Levionnois et al. 2021). In addition, a high vessel grouping index promotes interconnection between xylem vessels, enhancing hydraulic conductivity while mitigating embolism through increased redundancy (Zhang et al. 2025). Due to the limited number of species studied here, future studies with a large number of species, both mistletoe species and mistletoe–host species pairs, could provide more robust data to examine the relationships between these traits.

TLP was positively correlated with GCL and negatively associated with LS and SD in mistletoes (Figure 5b–d; see Tables S5 and S6 available as Supplementary data at *Tree Physiology* Online). Previous studies have shown that plants regulate water transpiration by controlling stomatal opening and closing, which enables them to maintain turgor pressure under lower water conditions and delay the onset of TLP (Farrell et al. 2017, Zhu et al. 2018, Da Sois et al. 2024). LS and SD are known to influence plant transpiration rates (Xu et al. 2019). Smaller leaves and lower SD of mistletoes contribute to reduced transpiration at the individual level and the maintenance of turgor pressure under low water conditions. Given that larger stomata close more slowly than smaller ones under low water conditions, the more negative TLP observed in mistletoes is crucial to maintain stomatal openness. Furthermore, LDMC has been found to correlate with drought resistance (Blumenthal et al. 2020). In mistletoes, LDMC was negatively correlated with SLA and D_{vein}, representing mechanical strength (Roth-Nebelsick et al. 2001, Wright et al. 2004). This suggests a coordinated adaptation of mistletoes to water deficits. In addition, SD was negatively correlated with GCL and positively associated with D_{vein} in mistletoes, aligning with previous findings in non-parasitic plants, suggesting a balance between water supply and demand (Brodribb and Jordan 2011, Carins Murphy et al. 2016).

The associations between leaf and stem traits were also observed in mistletoes, highlighting the interdependence of leaf and stem traits in response to environmental conditions. This is consistent with previous reports on non-parasitic plants (Reich and Cornelissen 2014, Carvajal et al. 2019). For instance, embolism resistance (P_{50}) was positively correlated with HSM_{tlp} and LDMC in both mistletoes and their hosts, while exhibiting negative associations with SLA and D_{vein} in mistletoes. These findings suggest that mistletoes coordinate stem embolism resistance, leaf water storage, LS and leaf vascular structure to better survive their canopy habitats. These findings align with previous research in non-parasitic

plants (Markesteijn et al. 2010), indicating a coordinated response between leaf and stem traits to cope with water deficits. Interestingly, no correlation was found between P_{50} and TLP in either group, which suggests that leaf turgor maintenance, a key trait in leaf drought tolerance, may not directly influence stem embolism resistance. In addition, K_S was negatively correlated with TLP and HV in mistletoes, which is consistent with the findings of Mencuccini et al. (2019) in a global compilation of over 1000 species. This suggests that a compensatory mechanism exists in mistletoes to maintain hydraulic supply to leaves (Mencuccini et al. 2019). A significant positive correlation was also found between K_S and SD in both mistletoes and their hosts, suggesting a coordinated relationship between stomatal regulation and branch hydraulic conductivity (Ferdous et al. 2023, Hernandez-Santana et al. 2023). Collectively, the relationships between leaf and stem traits highlight the complex interplay between physiological process, enabling mistletoes to effectively uptake water and nutrients from their hosts. This reinforces the adaptive strategies employed by mistletoes to thrive in their canopy habitat with an aerial parasitical lifestyle.

Conclusions

This study presents the first comprehensive comparison of stem and leaf functional traits associated with hydraulics and drought resistance between mistletoes and their hosts, revealing both convergent and divergent water use and drought resistance strategies. While mistletoes and their hosts show high resistance to drought-induced xylem embolism, mistletoes exhibit more drought tolerance such as lower Ψ_{mid}, TLP and P_{12}, demonstrating adaptations to high xylem-tension environments (lower water potentials) and relatively high VPD conditions in the upper portions of the host canopy where mistletoes are typically located, compared with the lower portions occupied by their hosts. Interestingly, mistletoes demonstrate profligate water use, as indicated by more negative $\delta^{13}C$ values, in spite of lower hydraulic efficiency. Notably, no overall trade-off between hydraulic efficiency and safety was found in both mistletoes and their hosts. The close coordination of stem and leaf functional traits in mistletoes helps balance water supply and transpiration demand. In addition, this study demonstrates that mistletoes exhibit significant plasticity in their hydraulic traits, with host species playing a crucial role in shaping these traits. This could provide mistletoes with a unique survival advantage, making them more resilient to environmental stress such as drought. Future studies such as controlled drought experiments could improve our understanding of the physiological mechanisms behind their response to drought and help predict the host–mistletoe interactions under climate change.

Acknowledgments

We are grateful to Ren-Bin Zhu of Xishuangbanna Tropical Botanical Garden for species identification. The Center for Gardening and Horticulture, Xishuangbanna Tropical Botanical Garden, Chinese Academy of Sciences for sample collection permit.

Supplementary Data

Supplementary data for this article are available at *Tree Physiology* Online.

Author contributions

X.-Y.H., Y.-B.Z. and J.-L.Z. designed the experiment; X.-Y.H. and W.-H.L. collected the data; X.-Y.H., Y.-B.Z. and J.-L.Z. analyzed the data; and X.-Y.H., Y.-B.Z., Y.-J.Z. and J.-L.Z. led the writing. All authors contributed critically to the drafts and gave final approval for publication.

Conflict of interest

None declared.

Funding

This work was financially supported by the National Natural Science Foundation of China (32301308, 32171507), the Yunnan Fundamental Research Projects (202401AT070230, 202501AT070252), the Yunnan Revitalization Talents Support Program and the 14th Five-Year Plan of the Xishuangbanna Tropical Botanical Garden, CAS (XTBG-1450101). We thank Ren-Bin Zhu for species identification, and the Center for Gardening and Horticulture, Xishuangbanna Tropical Botanical Garden, Chinese Academy of Sciences for collection permit. We thank three reviewers for their insightful comments, which greatly improved this manuscript.

Data availability

Data and materials supporting the findings of this study are available from the corresponding author under reasonable request.

References

Amutenya A, Kwembeya E, Shikangalah R, Tsvuura Z (2023) Photosynthesis, chlorophyll content and water potential of a mistletoe-host pair in a semi-arid savanna. S Afr J Bot 163:311–315. https://doi.org/10.1016/j.sajb.2023.10.053.

Anderegg LDL, Berner LT, Badgley G, Sethi ML, Law BE, HilleRisLambers J (2018) Within-species patterns challenge our understanding of the leaf economics spectrum. Ecol Lett 21:734–744. https://doi.org/10.1111/ele.12945.

Anderegg WRL, Trugman AT, Badgley G, Konings AG, Shaw J (2020) Divergent forest sensitivity to repeated extreme droughts. Nat Clim Change 10:1091–1095. https://doi.org/10.1038/s41558-020-00919-1.

Aritsara ANA, Ni M-Y, Wang Y-Q, Yan C-L, Zeng W-H, Song H-Q, Cao K-F, Zhu S-D (2023) Tree growth is correlated with hydraulic efficiency and safety across 22 tree species in a subtropical karst forest. Tree Physiol 43:1307–1318. https://doi.org/10.1093/treephys/tpad050.

Bartlett MK, Scoffoni C, Ardy R, Zhang Y, Sun S, Cao K, Sack L (2012) Rapid determination of comparative drought tolerance traits: using an osmometer to predict turgor loss point. Methods Ecol Evol 3:880–888. https://doi.org/10.1111/j.2041-210X.2012.00230.x.

Bates D, Mächler M, Bolker B, Walker S (2015) Fitting linear mixed-effects models using lme4. J Stat Softw 67:1–48 https://doi.org/10.18637/jss.v067.i01.

Bauman D, Fortunel C, Delhaye G et al. (2022) Tropical tree mortality has increased with rising atmospheric water stress. Nature 608:528–533. https://doi.org/10.1038/s41586-022-04737-7.

Bell DM, Pabst RJ, Shaw DC (2020) Tree growth declines and mortality were associated with a parasitic plant during warm and dry climatic conditions in a temperate coniferous forest ecosystem. Glob Chang Biol 26:1714–1724. https://doi.org/10.1111/gcb.14834.

Blumenthal DM, Mueller KE, Kray JA, Ocheltree TW, Augustine DJ, Wilcox KR (2020) Traits link drought resistance with herbivore defence and plant economics in semi-arid grasslands: the central roles of phenology and leaf dry matter content. J Ecol 108:2336–2351. https://doi.org/10.1111/1365-2745.13454.

Brodribb TJ, Jordan GJ (2011) Water supply and demand remain balanced during leaf acclimation of *Nothofagus cunninghamii* trees. New Phytol 192:437–448. https://doi.org/10.1111/j.1469-8137.2011.03795.x.

Bucci SJ, Scholz FG, Goldstein G, Meinzer FC, Sternberg LDSL (2003) Dynamic changes in hydraulic conductivity in petioles of two savanna tree species: factors and mechanisms contributing to the refilling of embolized vessels. Plant Cell Environ 26:1633–1645. https://doi.org/10.1046/j.0140-7791.2003.01082.x.

Cao M, Zou X, Warren M, Zhu H (2006) Tropical forests of Xishuangbanna, China. Biotropica 38:306–309. https://doi.org/10.1111/j.1744-7429.2006.00146.x.

Carins Murphy MR, Jordan GJ, Brodribb TJ (2016) Cell expansion not cell differentiation predominantly co-ordinates veins and stomata within and among herbs and woody angiosperms grown under sun and shade. Ann Bot 118:1127–1138. https://doi.org/10.1093/aob/mcw167.

Carter JL, White DA (2009) Plasticity in the Huber value contributes to homeostasis in leaf water relations of a mallee eucalypt with variation to groundwater depth. Tree Physiol 29:1407–1418. https://doi.org/10.1093/treephys/tpp076.

Carvajal DE, Loayza AP, Rios RS, Delpiano CA, Squeo FA (2019) A hyper-arid environment shapes an inverse pattern of the fast-slow plant economics spectrum for above-, but not below-ground resource acquisition strategies. J Ecol 107:1079–1092. https://doi.org/10.1111/1365-2745.13092.

Chave J, Coomes D, Jansen S, Lewis SL, Swenson NG, Zanne AE (2009) Towards a worldwide wood economics spectrum. Ecol Lett 12:351–366. https://doi.org/10.1111/j.1461-0248.2009.01285.x.

Chen L-Z, Huang L, Li X-F, You S, Yang S-C, Zhang Y-H, Wang W-Q (2013) Water and nutrient relationships between a mistletoe and its mangrove host under saline conditions. Funct Plant Biol 40: 475–483. https://doi.org/10.1071/FP12218.

Chen Y-J, Maenpuen P, Zhang Y-J, Barai K, Katabuchi M, Gao H, Kaewkamol S, Tao L-B, Zhang J-L (2021) Quantifying vulnerability to embolism in tropical trees and lianas using five methods: can discrepancies be explained by xylem structural traits? New Phytol 229:805–819. https://doi.org/10.1111/nph.16927.

Crates R, Watson D, Albery G et al. (2022) Mistletoes could moderate drought impacts on birds, but are themselves susceptible to drought-induced dieback. Proc R Soc B Biol Sci 289:1471–2954. https://doi.org/10.1098/rspb.2022.0358.

Da Sois L, Mencuccini M, Castells E, Sanchez-Martinez P, Martínez-Vilalta J (2024) How are physiological responses to drought modulated by water relations and leaf economics' traits in woody plants? Agric Water Manag 291:108613. https://doi.org/10.1016/j.agwat.2023.108613.

Dai A (2013) Increasing drought under global warming in observations and models. Nat Clim Change 3:52–58. https://doi.org/10.1038/nclimate1633.

de Andrés EG, Gazol A, Querejeta JI, Colangelo M, Camarero JJ (2024) Mistletoe-induced carbon, water and nutrient imbalances are imprinted on tree rings. Tree Physiol 44:tpae106. https://doi.org/10.1093/treephys/tpae106.

Duursma R, Choat B (2017) Fitplc—an R package to fit hydraulic vulnerability curves. J Plant Hydrol 4:e-002. 10.20870/jph.2017.e002.

Ewers FW, Fisher JB (1989) Techniques for measuring vessel lengths and diameters in stems of woody-plants. Am J Bot 76:645–656. https://doi.org/10.1002/j.1537-2197.1989.tb11360.x.

Fajardo A, Piper FI, García-Cervigón AI (2022) The intraspecific relationship between wood density, vessel diameter and other traits across environmental gradients. Funct Ecol 36:1585–1598. https://doi.org/10.1111/1365-2435.14069.

Farrell C, Szota C, Arndt SK (2017) Does the turgor loss point characterize drought response in dryland plants? Plant Cell Environ 40: 1500–1511. https://doi.org/10.1111/pce.12948.

Ferdous J, Islam M, Rahman M (2023) The role of tree size, wood anatomical and leaf stomatal traits in shaping tree hydraulic efficiency and safety in a south Asian tropical moist forest. Glob Ecol Conserv 43:e02453. https://doi.org/10.1016/j.gecco.2023.e02453.

Fontúrbel FE, Lara A, Lobos D, Little C (2018) The cascade impacts of climate change could threaten key ecological interactions. Ecosphere 9:e02485. https://doi.org/10.1002/ecs2.2485.

Fu P-L, Jiang Y-J, Wang A-Y, Brodribb TJ, Zhang J-L, Zhu S-D, Cao K-F (2012) Stem hydraulic traits and leaf water-stress tolerance are co-ordinated with the leaf phenology of angiosperm trees in an Asian tropical dry karst forest. Ann Bot 110:189–199. https://doi.org/10.1093/aob/mcs092.

Glatzel G, Geils B (2009) Mistletoe ecophysiology: host-parasite interactions. Botany 87:10–15. https://doi.org/10.1139/B08-096.

Gleason SM, Westoby M, Jansen S et al. (2016) Weak tradeoff between xylem safety and xylem-specific hydraulic efficiency across the world's woody plant species. New Phytol 209:123–136. https://doi.org/10.1111/nph.13646.

Goldstein G, Rada F, Sternberg L et al. (1989) Gas exchange and water balance of a mistletoe species and its mangrove hosts. Oecologia 78: 176–183. https://doi.org/10.1007/BF00377153.

Griebel A, Metzen D, Pendall E, Nolan RH, Clarke H, Renchon AA, Boer MM (2022) Recovery from severe mistletoe infection after heat- and drought-induced mistletoe death. Ecosystems 25:1–16. https://doi.org/10.1007/s10021-021-00635-7.

Griebel A, Watson D, Pendall E (2017) Mistletoe, friend and foe: synthesizing ecosystem implications of mistletoe infection. Environ Res Lett 12:115012. https://doi.org/10.1088/1748-9326/aa8fff.

Griebel A, Peters JMR, Metzen D et al. (2021) Tapping into the physiological responses to mistletoe infection during heat and drought stress. Tree Physiol 42:523–536. https://doi.org/10.1093/treephys/tpab113.

Haverroth EJ, Rimer IM, Oliveira LA, de Lima LGA, Cesarino I, Martins SCV, McAdam SAM, Cardoso AA (2024) Gradients in embolism resistance within stems driven by secondary growth in herbs. Plant Cell Environ 47:2986–2998. https://doi.org/10.1111/pce.14921.

Haynes AF (2021) What do we know about parasitic plants and the leaf economic spectrum? J Plant Ecol 15:691–699. https://doi.org/10.1093/jpe/rtab113.

He X-F, Wang S-W, Körner C, Yang Y (2021) Water and nutrient relations of mistletoes at the drought limit of their hosting evergreen oaks in the semiarid upper Yangtze region, SW China. Trees 35: 387–394. https://doi.org/10.1007/s00468-020-02039-x.

Hernandez-Santana V, Rodriguez-Dominguez CM, Sebastian-Azcona J, Perez-Romero LF, Diaz-Espejo A (2023) Role of hydraulic traits in stomatal regulation of transpiration under different vapour pressure deficits across five Mediterranean tree crops. J Exp Bot 74: 4597–4612. https://doi.org/10.1093/jxb/erad157.

Hetherington AM, Woodward FI (2003) The role of stomata in sensing and driving environmental change. Nature 424:901–908. https://doi.org/10.1038/nature01843.

Jin Y, Hao G-Y, Hammond WM, Yu K, Liu X-R, Ye Q, Zhou Z-H, Wang C-K (2023) Aridity-dependent sequence of water potentials for stomatal closure and hydraulic dysfunctions in woody plants. Glob Change Biol 29:2030–2040. https://doi.org/10.1111/gcb.16605.

Kotowska M, Hertel D, Abou Rajab Y, Barus H, Schuldt B (2015) Patterns in hydraulic architecture from roots to branches in six tropical tree species from cacao agroforestry and their relation to wood density and stem growth. Front Plant Sci 36:191. https://doi.org/10.3389/fpls.2015.00191.

Lamy JB, Delzon S, Bouche PS, Alia R, Vendramin GG, Cochard H, Plomion C (2014) Limited genetic variability and phenotypic plasticity detected for cavitation resistance in a Mediterranean pine. New Phytol 201:874–886. https://doi.org/10.1111/nph.12556.

Lawson T, Blatt MR (2014) Stomatal size, speed, and responsiveness impact on photosynthesis and water use efficiency. Plant Physiol 164:1556–1570. https://doi.org/10.1104/pp.114.237107.

Lê S, Josse J, Husson F (2008) FactoMineR: an R package for multivariate analysis. J Stat Softw 25:1–18. https://doi.org/10.18637/jss.v025.i01.

Levionnois S, Jansen S, Wandji RT et al. (2021) Linking drought-induced xylem embolism resistance to wood anatomical traits in Neotropical trees. New Phytol 229:1453–1466. https://doi.org/10.1111/nph.16942.

Liang X, Ye Q, Liu H, Brodribb TJ (2021) Wood density predicts mortality threshold for diverse trees. New Phytol 229:3053–3057. https://doi.org/10.1111/nph.17117.

Liu H, Ye Q, Gleason SM, He P, Yin D (2021) Weak tradeoff between xylem hydraulic efficiency and safety: climatic seasonality matters. New Phytol 229:1440–1452. https://doi.org/10.1111/nph.16940.

Liu X, Zhou S, Hu J et al. (2024) Variations and trade-offs in leaf and culm functional traits among 77 woody bamboo species. BMC Plant Biol 24:1–13. https://doi.org/10.1186/s12870-024-05108-2.

Lobo A, Torres-Ruiz JM, Burlett R et al. (2018) Assessing inter- and intraspecific variability of xylem vulnerability to embolism in oaks. For Ecol Manage 424:53–61. https://doi.org/10.1016/j.foreco.2018.04.031.

Luo Y, Sui Y, Gan J, Zhang L (2015) Host compatibility interacts with seed dispersal to determine small-scale distribution of a mistletoe in Xishuangbanna, Southwest China. J Plant Ecol 9:77–86. https://doi.org/10.1093/jpe/rtv024.

Maponga TS, Ndagurwa HGT, Witkowski ETF (2021) Functional and species composition of understory plants varies with mistletoe-infection on *Vachellia karroo* trees in a semi-arid African savanna. Glob Ecol Conserv 32:e01897. https://doi.org/10.1016/j.gecco.2021.e01897.

Markesteijn L, Poorter L, Paz H, Sack L, Bongers F (2010) Ecological differentiation in xylem cavitation resistance is associated with stem and leaf structural traits. Plant Cell Environ 34:137–148. https://doi.org/10.1111/j.1365-3040.2010.02231.x.

Mellado A, Morillas L, Gallardo A, Zamora R (2016) Temporal dynamic of parasite-mediated linkages between the forest canopy and soil processes and the microbial community. New Phytol 211:1382–1392. https://doi.org/10.1111/nph.13984.

Mellado A, Zamora R, Rafferty N (2019) Ecological consequences of parasite host shifts under changing environments: more than a change of partner. J Ecol 108:788–796. https://doi.org/10.1111/1365-2745.13295.

Mencuccini M, Rosas T, Rowland L et al. (2019) Leaf economics and plant hydraulics drive leaf: wood area ratios. New Phytol 224:1544–1556. https://doi.org/10.1111/nph.15998.

Meunier F, Krishna Moorthy SM, De Deurwaerder HPT, Kreus R, Van den Bulcke J, Lehnebach R, Verbeeck H (2020) Within-site variability of liana wood anatomical traits: a case study in Lausat, French Guiana. Forests 11:523. https://doi.org/10.3390/f11050523.

Moser L, Fonti P, Büntgen U, Esper J, Luterbacher J, Franzen J, Frank D (2010) Timing and duration of European larch growing season along altitudinal gradients in the Swiss alps. Tree Physiol 30:225–233. https://doi.org/10.1093/treephys/tpp108.

Nardini A, Lo Gullo MA, Salleo S (2011) Refilling embolized xylem conduits: is it a matter of phloem unloading? Plant Sci 180:604–611. https://doi.org/10.1016/j.plantsci.2010.12.011.

Ndagurwa HGT, Maponga TS, Muvengwi J (2020) Mistletoe litter accelerates the decomposition of recalcitrant host litter in a semi-arid savanna, south-West Zimbabwe. Austral Ecol 45:1080–1092. https://doi.org/10.1111/aec.12935.

Pérez-Ramos IM, Matías L, Gómez-Aparicio L, Godoy Ó (2019) Functional traits and phenotypic plasticity modulate species coexistence across contrasting climatic conditions. Nat Commun 10:2555. https://doi.org/10.1038/s41467-019-10453-0.

R Core Team (2024) R: A language and environment for statistical computing. R Foundation for Statistical Computing, Vienna, Austria.

Reich PB, Cornelissen H (2014) The world-wide 'fast-slow' plant economics spectrum: a traits manifesto. J Ecol 102:275–301. https://doi.org/10.1111/1365-2745.122.

Richards JH, Henn JJ, Sorenson QM, Adams MA, Smith DD, McCulloh KA, Givnish TJ (2021) Mistletoes and their eucalypt hosts differ in the response of leaf functional traits to climatic moisture supply. Oecologia 195:759–771. https://doi.org/10.1007/s00442-021-04867-1.

Rossi S, Anfodillo T, Menardi R (2006) Trephor: a new tool for sampling microcores from tree stems. IAWA J 27:89–97. https://doi.org/10.1163/22941932-90000139.

Roth-Nebelsick A, Uhl D, Mosbrugger V, Kerp H (2001) Evolution and function of leaf venation architecture: a review. Ann Bot 87:553–566. https://doi.org/10.1006/anbo.2001.1391.

Savi T, Tintner J, Da Sois L, Grabner M, Petit G, Rosner S, Phillips N (2019) The potential of mid-infrared spectroscopy for prediction of wood density and vulnerability to embolism in woody angiosperms. Tree Physiol 39:503–510. https://doi.org/10.1093/treephys/tpy112.

Sayad E, Boshkar E, Gholami S (2017) Different role of host and habitat features in determining spatial distribution of mistletoe infection. For Ecol Manage 384:323–330. https://doi.org/10.1016/j.foreco.2016.11.012.

Scalon MC, Wright IJ (2015) A global analysis of water and nitrogen relationships between mistletoes and their hosts: broad-scale tests of old and enduring hypotheses. Funct Ecol 29:1114–1124. https://doi.org/10.1111/1365-2435.12418.

Shen Y, Umaña MN, Li W, Fang M, Chen Y, Lu H, Yu S (2019) Coordination of leaf, stem and root traits in determining seedling mortality in a subtropical forest. For Ecol Manage 446:285–292. https://doi.org/10.1016/j.foreco.2019.05.032.

Skelton RP, West AG, Dawson TE (2015) Predicting plant vulnerability to drought in biodiverse regions using functional traits. Proc Natl Acad Sci U S A 112:5744–5749. https://doi.org/10.1073/pnas.1503376112.

Skelton RP, Anderegg LDL, Papper P, Reich E, Dawson TE, Kling M, Thompson SE, Diaz J, Ackerly DD (2019) No local adaptation in leaf or stem xylem vulnerability to embolism, but consistent vulnerability segmentation in a north American oak. New Phytol 223:1296–1306. https://doi.org/10.1111/nph.15886.

Skelton RP, Anderegg LDL, Diaz J, Kling MM, Papper P, Lamarque LJ, Delzon S, Dawson TE, Ackerly DD (2021) Evolutionary relationships between drought-related traits and climate shape large hydraulic safety margins in western north American oaks. Proc Natl Acad Sci U S A 118:e2008987118. https://doi.org/10.1073/pnas.2008987118.

Snyder KA, Robinson SA, Schmidt S, Hultine KR (2022) Stable isotope approaches and opportunities for improving plant conservation. Conserv Physiol 10:coac056. https://doi.org/10.1093/conphys/coac056.

Sperry JS, Donnelly JR, Tyree MT (1988) A method for measuring hydraulic conductivity and embolism in xylem. Plant Cell Environ 11:35–40. https://doi.org/10.1111/j.1365-3040.1988.tb01774.x.

Sterck FJ, Zweifel R, Sass-Klaassen U, Chowdhury Q (2008) Persisting soil drought reduces leaf specific conductivity in scots pine (*Pinus sylvestris*) and pubescent oak (*Quercus pubescens*). Tree Physiol 28:529–536. https://doi.org/10.1093/treephys/28.4.529.

Teixeira-Costa L (2021) A living bridge between two enemies: haustorium structure and evolution across parasitic flowering plants. Braz J Bot 44:165–178. https://doi.org/10.1007/s40415-021-00704-0.

Teixeira-Costa L, Heberling JM, Wilson CA, Davis CC (2023) Parasitic flowering plant collections embody the extended specimen. Methods Ecol Evol 14:319–331. https://doi.org/10.1111/2041-210X.13866.

Těšitel J, Li A-R, Knotková K, McLellan R, Bandaranayake PCG, Watson DM (2021) The bright side of parasitic plants: what are they good for? Plant Physiol 185:1309–1324. https://doi.org/10.1093/plphys/kiaa069.

Torres-Ruiz JM, Jansen S, Choat B et al. (2014) Direct x-ray microtomography observation confirms the induction of embolism upon xylem cutting under tension. Plant Physiol 167:40–43. https://doi.org/10.1104/pp.114.249706.

Tyree M, Zimmermann M (2002) Xylem structure and the ascent of sap. Springer, Berlin.
Urban J, Gebauer R, Nadezhdina N, Čermák J (2012) Transpiration and stomatal conductance of mistletoe (*Loranthus europaeus*) and its host plant, downy oak (*Quercus pubescens*). Biologia 67:917–926. https://doi.org/10.2478/s11756-012-0080-3.
Urli M, Porté AJ, Cochard H, Guengant Y, Burlett R, Delzon S (2013) Xylem embolism threshold for catastrophic hydraulic failure in angiosperm trees. Tree Physiol 33:672–683. https://doi.org/10.1093/treephys/tpt030.
van der Sande MT, Poorter L, Schnitzer SA, Engelbrecht BMJ, Markesteijn L (2019) The hydraulic efficiency-safety trade-off differs between lianas and trees. Ecology 100:e02666. https://doi.org/10.1002/ecy.2666.
Violle C, Navas M-L, Vile D, Kazakou E, Fortunel C, Hummel I, Garnier E (2007) Let the concept of trait be functional! Oikos 116:882–892. https://doi.org/10.1111/j.0030-1299.2007.15559.x.
Warton DI, Duursma RA, Falster DS, Taskinen S (2012) Smatr 3—an R package for estimation and inference about allometric lines. Methods Ecol Evol 3:257–259. https://doi.org/10.1111/j.2041-210X.2011.00153.x.
Watson DM, Herring M (2012) Mistletoe as a keystone resource: an experimental test. Proc R Soc B Biol Sci 279:3853–3860. https://doi.org/10.1098/rspb.2012.0856.
Watson DM, McLellan RC, Fontúrbel FE (2022) Functional roles of parasitic plants in a warming world. Annu Rev Ecol Evol Syst 53:25–45. https://doi.org/10.1146/annurev-ecolsys-102320-115331.
Westoby M, Falster DS, Moles AT, Vesk PA, Wright IJ (2002) Plant ecological strategies: some leading dimensions of variation between species. Annu Rev Ecol Evol Syst 33:125–159. https://doi.org/10.1146/annurev.ecolsys.33.010802.150452.
Wheeler JK, Huggett BA, Tofte AN, Rockwell FE, Holbrook NM (2013) Cutting xylem under tension or supersaturated with gas can generate PLC and the appearance of rapid recovery from embolism. Plant Cell Environ 36:1938–1949. https://doi.org/10.1111/pce.12139.
Wortemann R, Herbette S, Barigah TS, Fumanal B, Alia R, Ducousso A, Gomory D, Roeckel-Drevet P, Cochard H (2011) Genotypic variability and phenotypic plasticity of cavitation resistance in *Fagus sylvatica* L. across Europe. Tree Physiol 31:1175–1182. https://doi.org/10.1093/treephys/tpr101.
Wright IJ, Reich PB, Westoby M et al. (2004) The worldwide leaf economics spectrum. Nature 428:821–827. https://doi.org/10.1038/nature02403.
Wright IJ, Ackerly DD, Bongers F et al. (2007) Relationships among ecologically important dimensions of plant trait variation in seven neotropical forests. Ann Bot 99:1003–1015. https://doi.org/10.1093/aob/mcl066.
Xu K, Guo L, Ye H (2019) A naturally optimized mass transfer process: the stomatal transpiration of plant leaves. J Plant Physiol 234:138–144. https://doi.org/10.1016/j.jplph.2019.02.004.
Yang D, Goldstein G, Wang M, Zhang W-W, Wang A-Y, Liu Y-Y, Hao G-Y (2017) Microenvironment in the canopy rivals the host tree water status in controlling sap flow of a mistletoe species. Tree Physiol 37:501–510. https://doi.org/10.1093/treephys/tpx018.
Ye H-Y, Zhao W-L, Li Y-Q, Chen X, Zhang Y-X, Zhao P (2021) Different effects of hemi-parasite *Taxillus chinensis* on water transport of its host angiosperms and gymnosperms trees. Flora 285:151955. https://doi.org/10.1016/j.flora.2021.151955.
Zhang G-F, Li Q, Sun S (2018) Diversity and distribution of parasitic angiosperms in China. Ecol Evol 8:4378–4386. https://doi.org/10.1002/ece3.3992.
Zhang L, Chen Y, Ma K, Bongers F, Sterck FJ (2019) Fully exposed canopy tree and liana branches in a tropical forest differ in mechanical traits but are similar in hydraulic traits. Tree Physiol 39:1713–1724. https://doi.org/10.1093/treephys/tpz070.
Zhang X-L, Ma S-W, Hu H, Li F-L, Bao W-K, Huang L (2024) A trade-off between leaf hydraulic efficiency and safety across three xerophytic species in response to increased rock fragment content. Tree Physiol 44:tpae010. https://doi.org/10.1093/treephys/tpae010.
Zhang Y-B, Yang D, Zhang K-Y, Bai X-L, Wang Y-S-D, Wu H-D, Ding L-Z, Zhang Y-J, Zhang J-L (2022) Higher water and nutrient use efficiencies in savanna than in rainforest lianas result in no difference in photosynthesis. Tree Physiol 42:145–159. https://doi.org/10.1093/treephys/tpab099.
Zhang Y-B, Scalon MC, Liu J-X, Song X-Y, Yang D, Zhang Y-J, Ellsworth DS, Zhang J-L (2023) You are what you eat: nutrient and water relations between mistletoes and hosts. New Phytol 238:567–583. https://doi.org/10.1111/nph.18747.
Zhang Y-B, Huang X-Y, Scalon MC et al. (2025) Mistletoes have higher hydraulic safety but lower efficiency in xylem traits compared with their hosts. New Phytol 245:607–624. https://doi.org/10.1111/nph.20257.
Zhu H (2022) Vegetation diversity of Yunnan. J Southwest For Univ 42:1–12. https://doi.org/10.11929/j.swfu.202105007.
Zhu S-D, Song J-J, Li R-H, Ye Q (2013) Plant hydraulics and photosynthesis of 34 woody species from different successional stages of subtropical forests. Plant Cell Environ 36:879–891. https://doi.org/10.1111/pce.12024.
Zhu S-D, Chen Y-J, Ye Q, He P-C, Liu H, Li R-H, Fu P-L, Jiang G-F, Cao K-F (2018) Leaf turgor loss point is correlated with drought tolerance and leaf carbon economics traits. Tree Physiol 38:658–663. https://doi.org/10.1093/treephys/tpy013.
Zweifel R, Bangerter S, Rigling A, Sterck FJ (2012) Pine and mistletoes: how to live with a leak in the water flow and storage system? J Exp Bot 63:2565–2578. https://doi.org/10.1093/jxb/err432.

Tree Physiology, 2025, 45, tpaf071
https://doi.org/10.1093/treephys/tpaf071
Research paper